

Received 6 January 2025, accepted 20 January 2025, date of publication 28 January 2025, date of current version 7 February 2025.

Digital Object Identifier 10.1109/ACCESS.2025.3535677



# **Continuum and Soft Robots in Minimally Invasive Surgery: A Systematic Review**

FAHAD IQBAL<sup>®1</sup>, (Graduate Student Member, IEEE), MOJTABA ESFANDIARI<sup>®2</sup>, GOLCHEHR AMIRKHANI<sup>®2</sup>, HAMIDREZA HOSHYARMANESH<sup>®3</sup>, SANJU LAMA<sup>4,5</sup>, MAHDI TAVAKOLI<sup>®6</sup>, (Senior Member, IEEE), AND GARNETTE R. SUTHERLAND<sup>4,5</sup>

<sup>1</sup>Department of Cell Biology and Anatomy, University of Calgary, Calgary, AB T2N 1N4, Canada

Corresponding author: Fahad Iqbal (fahad.iqbal@ucalgary.ca)

This work was supported by Project neuroArm under Project 10027491.

**ABSTRACT** Faster recovery, reduced trauma, and improved patient outcomes drive innovations in minimally invasive surgery (MIS). Notwithstanding significant advancements, traditional MIS tools have been limited in navigating deep anatomical pathways and offering precise control at target sites. Continuum robotics has emerged as a solution, with recent developments enabling greater flexibility and maneuverability in surgical interventions. In this review, we first highlight recent developments in mechanical-continuum robots for traditional minimally invasive surgery and then summarize the current state-of-the-art in steerable catheter-based interventions. We discuss limitations to current approaches and explore the emerging potential of soft robots as a novel strategy to address the challenge of developing versatile, highly articulated flexible tools for minimally invasive surgical interventions. We hope that this review will, on the one hand, provide an introduction and resource for students and researchers alike, and on the other hand, will stimulate discussion vis-à-vis future directions in minimally invasive surgery.

**INDEX TERMS** Continuum robots, minimally invasive surgery, soft robots.

## I. INTRODUCTION

Innovation in robotics has revolutionized modern medicine. From the advent of hospital robotic assistants, to auxiliary robots that automate day-to-day tasks, to robots that provide support and companionship to patients [1], and robots that are at the front line in pandemics [2]; it is clear that these machines will continue to transform the face of healthcare. Over the last two decades, the role of robots in the operating theatre has become of increasing importance [3], with some machines acting as sophisticated stereotactic tools for neurosurgery [4], [5], [6], and others serving as advanced surgical systems that enable tele-microsurgery [7]. Driven by a need to improve patient outcomes, reduce trauma, and provide faster recovery times, the development and improvement of

The associate editor coordinating the review of this manuscript and approving it for publication was Tao Wang.

these machines has become crucial in providing less invasive interventions.

Advancement in surgical tool design has also enabled new minimally invasive surgical procedures to be conducted with increased ease and accuracy. In contrast to open surgery, minimally invasive surgery (MIS) typically involves long rigid inserted via small incisions or flexible tools introduced via natural orifices. As innovation continues, surgeons have accordingly transitioned to more sophisticated tools and procedures. For example, the advent of laparoscopic tools brought improved patient outcomes and promised a new frontline in what procedures were possible. As surgeons began the wide-spread shift towards MIS in the 1990's [8], both the scope and limitations of MIS became more apparent, and finding solutions to such limitations became a focus for researchers.

For one, the insertion of long, straight tools through small entry sites creates a fulcrum effect which limits tool mobility,

<sup>&</sup>lt;sup>2</sup>Mechanical Engineering Department, Laboratory for Computational Sensing and Robotics, Johns Hopkins University, Baltimore, MD 21218, USA

<sup>&</sup>lt;sup>3</sup>Questrom School of Business, Boston University, Boston, MA 02215, USA

<sup>&</sup>lt;sup>4</sup>Department of Clinical Neurosciences, University of Calgary, Calgary, AB T2N 4N1, Canada

<sup>&</sup>lt;sup>5</sup>Hotchkiss Brain Institute, University of Calgary, Calgary, AB T2N 4N1, Canada

<sup>&</sup>lt;sup>6</sup>Electrical and Computer Engineering Department, University of Alberta, Edmonton, AB T6G 1HQ, Canada



amplifies tremors, and inverts the surgeon's hand movements, thus making the procedures more difficult (**Fig. 1.**) [9], [10]. Further, MIS inherently brings with it reduced visibility and positional awareness, while the use of multiple instruments inserted from narrow corridors adds to an already constricted workspace. Finally, long, rigid tools introduce the risk of potential punctures and injuries to surrounding tissues and organs. Training surgeons to become proficient in MIS techniques presents yet another challenge [10], [11]. These limitations, amongst others, have driven researchers to bring change into the operating theatre, namely, with the increased integration of robotics.

As platforms such as the da Vinci Surgical System began to see increased usage [7], [12], it became apparent that robots could provide a unique platform to help solve the above limitations. With that, the possibility of flexible, miniaturized, and highly controllable robots that can actively navigate complex environments has become a primary focus in MIS. These systems, termed continuum robots, provide remarkable flexibility, control, and ability to navigate tortuous environments [13], [14]. Unlike traditional linkage-based devices that utilize individual joints in series, continuum robots can bend continuously along their lengths. Conceptually, these tools have infinite theoretical degrees of freedom (DOF) and can conform to any shape or position required for a task. Continuum robots provide a platform to create highly dexterous and dynamic tools which can stiffen or bend at selected points on command and may provide a solution to the current model in MIS [14], [15], [16], [17].

Notwithstanding these exciting innovations, significant limitations continue to exist. Specifically, forgoing rigid, straight tools for compliant ones brings the issue of strength and payload capacity. Further, accurately modeling robotic trafficking becomes increasingly complex with the type of robot, materials, and selected surgery [18], [19]. As various teams have tried to improve on these designs, developing increasingly smaller and stronger tools remains a challenge, perhaps partly due to the materials currently platforming these systems. A brief comparison of key operational characteristics of continuum robots and traditional straight line-of-sight tools is summarized in **Figure 1.** 

Consolidating a dialogue of these various tools is thus valuable to both engineers and physicians alike. Although substantial research has been conducted on these robots, a systematic analysis on their applications for MIS that covers systems from conventional to soft robots is required to consolidate and interpret the progress. Thus, the objective of this review is to provide an update and overview of the current state-of-the-art in continuum robots for MIS, and to initiate further discussion that may assist researchers in addressing existing constraints.

We begin by conducting a systematic review of the literature ranging from 2000 to 2024, across 4 databases. We then categorize different classes of continuum robots with regards to their design and actuation principles. We then cover general kinematics and modeling, discuss clinical applications of

various tool types and finally, examine the emerging role of soft robots as an avenue for further research.

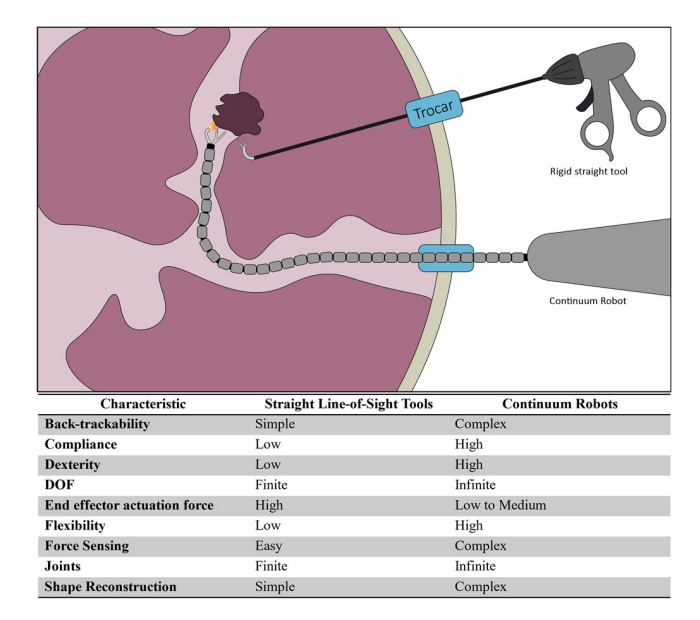


FIGURE 1. Comparison of continuum robots and traditional straight-line rigid tools. Traditional tools may need to navigate through more critical tissue to reach the target, while continuum robots could potentially allow for safer navigation.

## **II. LITERATURE SEARCH**

A systematic search across 4 databases, PubMed, Web of Science, IEEE, and Scopus, was conducted. The search parameters were kept consistent between databases. The search yielded a total of 1,564 results (Fig. 2.), after which appropriate articles were isolated, and duplicates were removed (619 unique results). When selecting relevant and unique studies, previous studies covering previous protypes or aspects of robot development were included – where possible. The search yielded 190 relevant studies, 39 supporting studies, and 151 relevant, unique projects (Fig. 2). The results of the search were then tabulated (Table S1), the salient aspects of which have been quantified below (Fig. 3). The inclusion and exclusion criteria are listed in Table 1. Due to the lack of a standardized method with which to compare these characteristics, we adapt the approach used by Runciman, Darzi, and Mylonas in their systematic review on soft robots [20] (Tables 1, 2, and S1). We attempt to streamline and consolidate our findings across conventional, and soft robots to provide an overview from the perspectives of physicians, engineers, mathematicians, and material scientists.

#### **III. CONTINUUM ROBOT ACTUATION PRINCIPLES**

Broadly, continuum robots can be classified as either extrinsically, or intrinsically actuated, each with their own implications that lend them to different applications and workspaces [14], [21], [22], [23]. At its core, extrinsic actuation moves the power of the robotic system to outside the continuum section. When compared to similar intrinsically



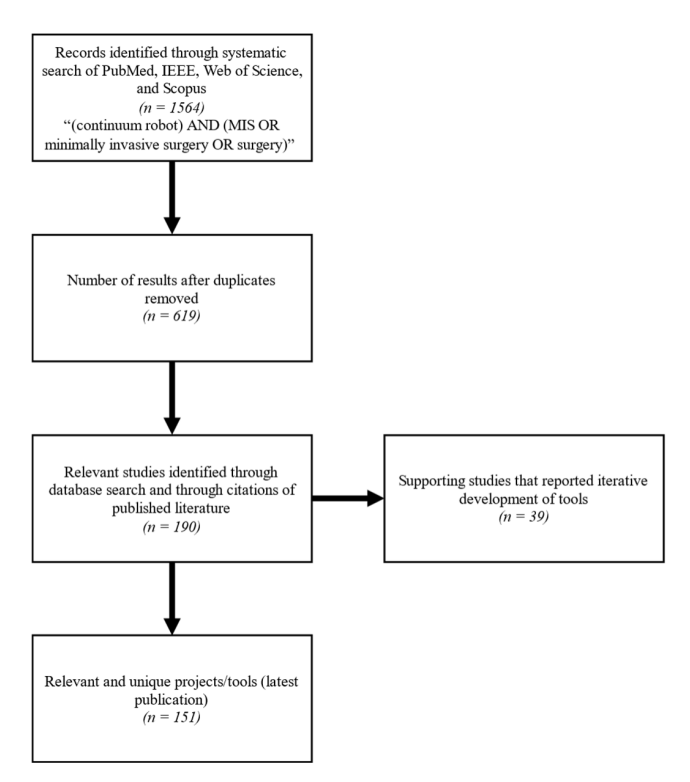


FIGURE 2. Flow-chart of systematic search, exclusion, inclusion, and organization of projects.

TABLE 1. Inclusion and exclusion criteria.

Inclusion	Exclusion
Articles introduced a novel robotic device and empirically demonstrated its function	Tool was not specifically intended for MIS
Articles were published from 2000 to 2024	Papers that do not show physical prototypes or products
Articles were accessible by the authors at the time of the search	The device was not sufficiently flexible and articulated
Articles were written in English	
The article's primary focus was the development of the robot for MIS	

actuated systems, these systems have larger actuator units that take up more workspace and have less articulated control of individual points of the continuum section. They are also more susceptible to friction and hysteresis [24], [25]. They compensate for these limitations by allowing for smaller tool diameters with an increased range of motion. On the other hand, the limitations of intrinsic actuation include larger tool diameters required to house internal motors or other actuators [25], [26], [27].

# A. EXTRINSICALLY ACTUATED

Traditionally, most extrinsically actuated systems have been classified as cable-driven, multi-backbone driven, or concentric tube systems. Cable-driven systems are the most prevalent (**Fig. 3.**) and commonly consist of a central flexible structure that houses channels for tool delivery and

TABLE 2. Characteristics noted per device.

Characteristic	Description		
Class	Structural nature of the robot. For example, continuum, or catheter.		
Actuation	Actuation techniques utilized by the robot. For example, tendon-driven, concentric tube, pneumatic, piezoelectric, hybrid, etc.		
Application	The specific MIS or related application for which the robot was designed. For example, cardiac valve delivery, transoral surgery, neurosurgery, etc.		
Dimensions	Length and diameter of the functional sections of the robot.		
Materials	Primary material used for structure and actuation. For example, nitinol cables, nitinol tubes, sucrose and coffee granules for stiffening, silicone-based pneumatic chambers, etc.		
Feedback Sensors	Sensors used to determine position and to assess the surgical site. For example, visual or magnetic as explicitly stated.		
Instrumentation Channels	Description of instrumentation and channels available.		
Payload/Force Exertion Capacity	Carrying capacity or force exertion reported by empirical testing where applicable.		
DoF	Description of the DoF of device or system, where available.		

appropriate cables for actuation (Table 3). These systems can contain either one or multiple flexible sections. Each section can be individually actuated by tendons which flank the central backbone and are fixed to secure checkpoints at specific points of the continuum robot. These cables provide considerable force and can steer the systems to desired angles, depending on the elasticity of the central backbone. To complement this, there is a need for flexible, yet strong biocompatible backbones. As noted by Burgner-Kahrs et al., when deciding on backbone materials, balancing a low Young's Modulus required for flexibility and strain threshold is important. Although using backbone material that has a high Young's Modulus and elastic strain limits is ideal, a compromise must be struck [14]. As a result, many research teams turn to nitinol for its flexibility, strength, and biocompatibility (**Table S1, 4**). For example, Qi et al.'s prototype cable-driven system used for investigating control and movement modeling of such robots provides a classic illustration of these mechanisms [28]. Similarly, another team developed a threesegmented cable-driven robot using a nitinol backbone [29]. A 2023 study demonstrated a two-segment tendon-driven robot coupled with translational motion by an external actuator module [30].

A natural evolution of this approach has been robots with multiple-backbones and auxiliary rods, which are individually actuated and provide increased push and pull functionality (**Table S1**). Some of these flanking rods can provide added stability and actively enable pushing of the system to actuate the device. This offers increased conformational capabilities and allows for control of different segments of the system.



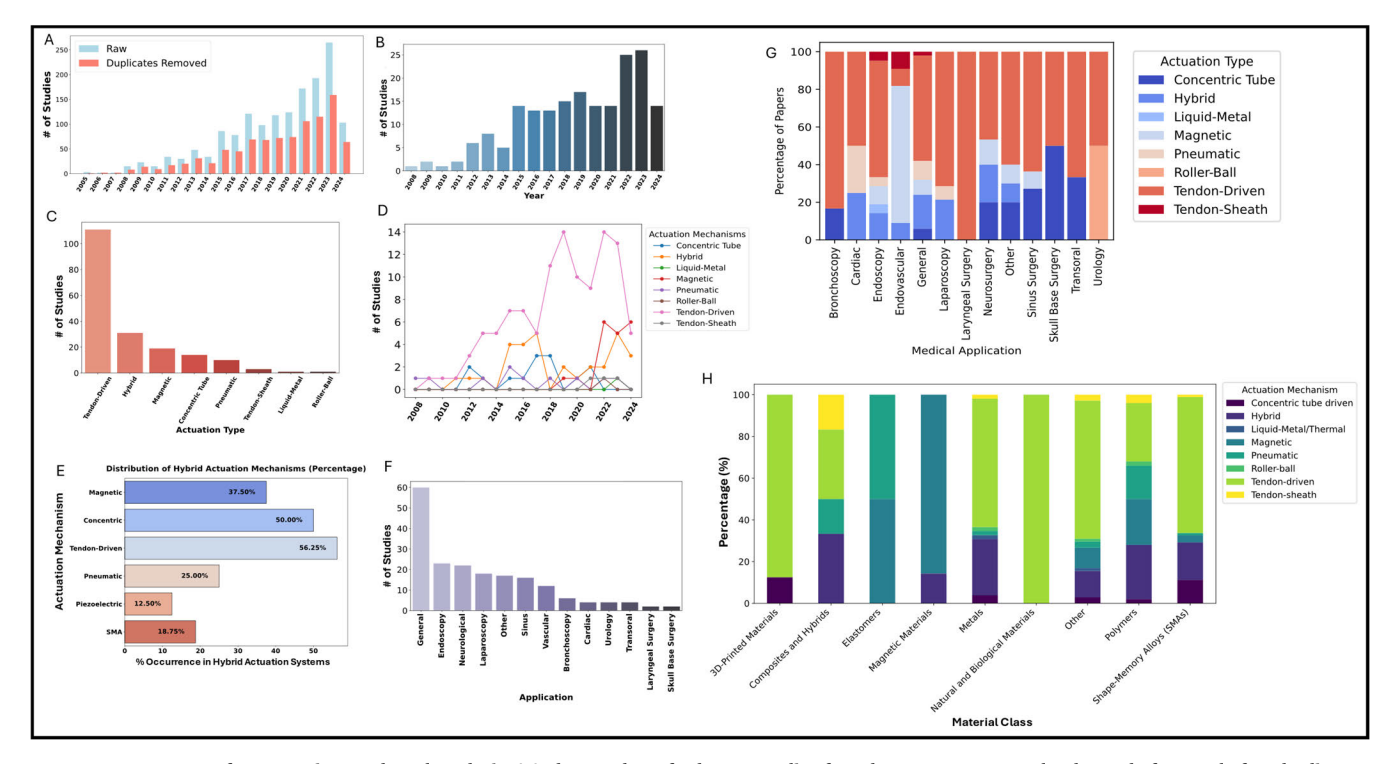


FIGURE 3. Summary of systematic search and analysis. (A) The number of relevant studies found per year across 4 databases before and after duplicates were removed. (B) The number of relevant studies identified per year. 2024\* indicates studies available in 2024 as of the writing of this review. (C) The number of studies indicating the use of a specific actuation mechanism. (D) Year-based trends in actuation mechanisms reported in identified studies. Hybrid refers to any study where more than one actuation mechanism was used, or a significant alteration to a conventional actuation mechanism provided properties similar to those exhibited by another actuation mechanism. (E) A quantified, inclusive breakdown of hybrid systems reveals how often certain actuation mechanisms were incorporated into such systems. (F) The stated application of the robot in the context of MIS. Where unspecified, the studies were labeled as General. (G) A quantified breakdown of actuation mechanisms reported for a specific MIS application. (H) Breakdown of materials involved in different actuation mechanisms. All plots are based on statistics from identified papers, rather than unique projects/robots.

Like backbones in cable-driven systems, these too commonly employ nitinol as the backbone material (**Table S1, 4**).

Modifications to cable-driven devices have led to creative and more modular devices with added capabilities. Some systems compound traditional cable-driven mechanisms with other types of systems to deliver the end-effector with increased accuracy and range of movement. Burgner-Kahrs' cable-based system contains extensible sections that leverage the capabilities of magnetic disks and concentric straight tubes to enable a unique follow-the-leader movement along the length of a continuum unit [31], [32].

This extensible tendon-driven robot can achieve follow-the-leader movement due to telescopic backbones and magnetic repulsion that produce consistent curvature signatures (Fig. 4A). Other notable examples include Yoon et al.'s maxillary sinus surgical system, which features two independent continuum robots that work off a spring-based backbone rather than a solid core to increase controllability and create an effective image-guided robot [33], [34]. Recently, Wang et al. combined a spring-based backbone with an offset nitinol rod for stability and increased bending control. This design allowed for more internal room to pass biopsy forceps in a small 4mm diameter design [35]. To enable tortional control, Zhang et al. leveraged concentric tendon-driven tubes

to both position the robot to the target and rotate within the scaffold of the outer tube [36].

Research teams have also been tackling the issue of reduced payload and force exertion by complementing cable-driven systems with various techniques. These "hybrid" systems have increased in representation over the past 10 years (Fig. 3). A 2018 study used both granular and layered jamming to stabilize a cable-driven robot for tool delivery in a mock nephrectomy [37]. Others have opted for a more integrated approach, using rolling joints to reduce device diameters, and to offer increased stability [38]. For this, integrating both geared teeth joints and rolling joints has been shown to be effective, being able to uphold a payload of 300 g from a 3.7mm diameter device [39]. Another team working on maxillary sinus surgery took advantage of a hybrid nitinol tube-based approach coupled with rolling joints to achieve increased bending angles and piecewise stiffness [40], [41] (**Fig. 4B**). Recently, the Auris Monarch<sup>TM</sup> platform has been deployed to the clinical setting and leverages a paired sheath and scope-cable mechanism to deliver a field of view in bronchoscopy interventions [42], [43], [44].

Various multi-backbone approaches have investigated parallel continuum setups that enable dynamically flexible characteristics that are otherwise incapable of such complex



paths [45]. Some of these devices combine multiple small incisions to facilitate transiting of an inserted continuum device to the surgical target site and have been coined as continuum reconfigurable parallel robots for surgery (CRISP) [46], [47] (Fig. 4C). Developing accurate and generalizable kinematic models for these systems is of increasing interest [48], [49], such as resolving shape deviations and better modeling changes in twisting and bending [50]. Although cable and rod-driven approaches seem to be the most direct solutions to providing accurate continuum robot manipulation, inherent limitations to traditional cable-driven approaches exist. Chief amongst these is that single cables can only actuate in one field and rely on compound systems to produce more complex shapes that would be beneficial in more tortuous environments. Secondly, traditional cables do not provide an opportunity for extensibility of specific sections. As a result, other mechanisms, such as the one mentioned above must be integrated [31], [32]. Another team recently used nitinol rods to actuate along a collapsible main structure, and thus enabled extendable continuum robotic control [51]. Nonetheless, cable-driven devices still offer a lightweight, relatively well-characterized, and predictable control paradigm that can be scaled into robots that have the potential to provide significant force output. Conversely, multi-backbone systems, which although provide improved navigational capabilities, are much more complex, more difficult to machine, and have increased internal space requirements.

On the other hand, concentric tube robots use elastic, pre-curved tubes, which are often made of nitinol and can have dramatically smaller diameters compared to their more conventional cable-driven and rod-driven counterparts (Table 3). Although not generally capable of eliciting the same full-length flexibility as most cable-driven solutions, these robots offer an interesting avenue for procedures that require long, thin tools to access surgical target sites with narrow workspaces [14], [52]. The concentric tubes are generally pre-shaped depending on the operational parameters and can be customized on a case-basis to allow sufficient range of motion for a procedure [53]. Each tube is individually actuated and can translate and rotate to affect the other tubes, and therefore the shape of the robot and position of the end effector [53]. As opposed to classic cable-driven systems, translation and rotation are an inherent quality of these devices, which provide benefits in special surgical tasks such as resections or knot-tying. Other advantages include simplicity of design, and manufacturing protocols. However, these tools intrinsically lack strength in tasks that require higher force output and introduce difficulties in bending through highly tortuous environments due to the accumulation of elastic strain under high load [54]. When combined with other mechanisms however, these tools have the potential to become remarkably more resourceful, albeit much more complicated [55]. Our search showed that this was one of the most commonly used actuation principles in hybrid systems, alongside tendon-driven systems (Fig. 3.)

Given this, there has been encouraging progress in recent years, with one team demonstrating the feasibility of their robot via tele-operated transoral surgery in a porcine larynx model [56], and others developing a three arm concentric tube robot system for nasopharyngeal carcinoma surgery [57]. More recently, a 3-robot setup was demonstrated for use for transnasal surgery for orbital tumors [58]. The extrinsic actuation housing was small and coverable, and the end effectors were successfully used to simulate tumor resection behind the eyes. Although concentric tube robots have traditionally not been associated with follow-the-leader movement, studies have reported special cases where this is possible [59], [60]. Others have detailed the expanded potential of concentric-tube devices in more general follow-the-leader possibilities [53]. Developing this capability would provide a valuable addition to this class's repertoire and offer more clinical incentive for this research. Teams have thus attempted to overcome this challenge by developing design frameworks that can better model follow-the-leader-like movement in delicate mock neurosurgical tasks [53].

Alternative actuation mechanisms for these robots also exist, such as magnetic resonance (MR)-guided piezoelectric concentric tube continuum devices [61], [62] and magnetic concentric tube robots [63]. As these are some of the latest design paradigms used in continuum robotics, there is still much potential for growth; with tool design and kinematic modeling as primary focuses in furthering our understanding. Another limitation of concentric tube systems is the possibility of snapping when there is increased strain between tubes [54]. This stored energy can be dangerous in sensitive and tight workspaces in the context of MIS. Researchers have thus increased focus on developing solutions in the design of these robots, and the path planning of the procedures to avoid the build-up of this potential energy [64]. One way researchers have attempted to resolve this is by optimizing laser-cut topography on the tubes, thus increasing elastic stability in the workspace [65]. Others have taken a different approach, using this strain potential to drive a suturing needle and thus demonstrating how in certain conditions, the added strength of the snap could be beneficial [66]. However, developing a robust understanding of the kinematic modeling of these snaps remains an ongoing task. Another hybrid approach offsets the neutral axis of its tubes by leveraging internal tubes with square notches [67], [68] (Fig. 4D). This provides a full-body push and pull property that is analogous to rod-actuated devices and enables increased range of motion while retaining the favorable characteristics of concentric tube designs.

# **B. INTRINSICALLY ACTUATED**

Intrinsically actuated systems offer a somewhat different paradigm, taking inspiration from traditional serial robots and steadily increasing the number of joints and motors such that they resemble continuum movement. To bypass this, and to develop true continuum robots, three main actuation



principles have been the most prominent: pneumatic, shape memory alloys, and hydraulic (Table S1). Other emerging techniques include the use of electroactive polymers such as elastomers. These design concepts have one key aspect in common, they are the first step in accommodating another characteristic that is beneficial for MIS: soft materials that can comply to their environment, and transit with less abrasion or injury to surrounding organs and tissue. The first of these techniques, pneumatic actuation, has been used for decades, with some of the first tools taking advantage of individually actuated McKibben muscles. These are pneumatic artificial muscles that can be applied in various methods to actuate both delicate and large industrial robots to control continuum devices [69], [70]. Pneumatically actuated devices have been developed to improve safety and versatility in various industrial applications due to their compliant nature [71]. In the realm of MIS, teams have investigated the potential of these pressurized chambers in actuating long continuum tools. One significant project, coined STIFF-FLOP (**Fig. 4E**), produced a robot with articulated pneumatic chambers and stiffening chambers that acted as an endoscope in a cadaveric mesorectal excision [72], [73], [74]. The robot contains a proximal and distal segment, which can be individually stabilized and extended to provide exceptional dexterity and view of the surgical site. Notwithstanding its highly articulated capabilities, this soft robot has till date been limited to endoscopic assignments, lacking the force exertion capacity to interact with tissue and organs to perform surgical tasks such as resection or suturing. To improve upon this, and to help the project evolve into one that can house and deliver instrumentation to the surgical site, recent papers have explored alternative approaches to enhance the robot's stiffening mechanisms via fiber jamming [19] and low-melting-point alloys [75]. Although much progress has been made, modelling a soft robot's interactions with surrounding tissue and kinematics remains an evolving field. A 2017 study is one of many that have attempted to address these requirements by detailing a screw-based method for modeling kinematics and statics of soft manipulators such as STIFF-FLOP [76]. This platform has proven effective for developing further models for tip force estimation [77], and miniaturization with radial expansion reinforcement [78].

Since then, various teams have made headway in better understanding pneumatically actuated continuum mechanics for MIS. One major approach to MIS involves the navigation of natural orifices, called natural orifice transluminal endoscopic surgery (NOTES). These procedures are meant to reduce invasiveness and patient trauma and require the use of highly dexterous manipulators that ideally would not damage the surrounding cavities. As such, pneumatic approaches have shown potential. A recent study used rubber bellows to actuate an endoscope for upper gastrointestinal navigation [79], [80]. Another study introduced a pneumatically actuated endoscope with promising capabilities for integration into more narrow procedural workflows [81]. The

device featured an elastic micro actuator with asymmetrically constructed walls to bend the robot in one direction. An important feature of pneumatically actuated devices is that unlike traditional cable-driven mechanisms, they allow a certain degree of extensibility to the robot. This may be crucial when repositioning of the full device may compromise tool stability and may damage the surrounding tissue.

Notwithstanding their exciting prospects, there are still some limitations. For one, pneumatic actuation is not as rapid or as responsive as cable-driven mechanisms. Another classic limitation is that they expand radially, which can be a restricting factor when working in narrow spaces for MIS. Some teams have adopted an integrated approach to mitigate this, by adding hollow chambers within the robot's structure wherein the device can expand [82], [83]. Although pneumatic micro actuators have relatively high power densities, they still require higher pressures to actuate large endoscopes and flexible tools, which may pose a risk to delicate organs in the event of a rupture [81], [84]. Fortunately, most systems function under 300 kPa and thus do not pose a significant risk [79], [81]. That said, other uses for inflatable chambers for flexible robots for MIS exist. For example, a 2015 study reported a hybrid cable-actuated device that employed an internal air tube for control of the end effector (in this case a gripper) [85]. This allowed for strong actuation forces and powerful gripping forces without expansion of the robotic arm. With their diverse applications, scalability, and power density, pneumatic continuum robots offer a promising avenue for further development of soft robots for MIS.

Another method pertains to using hydraulic chambers to actuate a tool to navigate the surgical site. Like pneumatic actuation, incompressible hydraulics provide high power density and have the potential to bridge the actuation strength gap between pneumatic and conventional cable-driven manipulators [84], [86]. Concerns about possible risks of leakage can be mitigated with the use of saline as the actuation fluid, thus preventing significant harm. The integration of hydraulic actuation for continuum manipulators for MIS has been limited, perhaps due to the added weight and difficulty in design. Examples do, however, exist. Lindenroth et al. showed a hydraulically actuated robotic design and took steps in understanding its force sensing and stiffness capabilities [86], [87]. Their robot consists of a silicone STIFF-FLOP module with three actuation chambers that, when activated, elongate rather than radially expand, allowing them both forward movement and a high degree of controllability with regards to bending the different segments. Their proposed finite element model for estimation of normal and shear forces at the robot tip provided valuable information regarding the usability of hydraulic actuation chambers in deriving fore sensation [86]. Another team took a different approach, looking into the potential of hydraulic actuation in low-cost soft endoscopy with automatic navigation capabilities [88]. Recently, a water jet actuated gastroscopy tool allowed for directional control by the controlled release of pressurized water [89]. Together,



pneumatic and hydraulic actuation of soft robots provide a tangible avenue for further investigation into the role of pressurized chambers to actuate continuum manipulators in MIS.

Soft continuum systems are sometimes accompanied with another intrinsic actuation method: shape memory alloys (SMAs). SMAs can "store" a heat-programmed shape and revert back to that shape after deformation once heated past a transformation temperature [90]. The most commonly used SMA in the context of MIS employ various compositions of nitinol, again due to its biocompatibility and elasticity [91]. As such, continuum devices that use these SMAs as extensors can heat pre-coiled or pre-deformed nitinol tubes to return to their original conformations to extend, contract, or bend the device. This property enables several key characteristics that are beneficial for MIS such as the facilitation of peristaltic movement of hybrid SMA devices [92]. The soft robotic prototype shown in (Fig. 4F) uses nine independently controlled SMA springs that are heated and cooled with the assistance of air tubes to actuate disks that interspace the three-segment robot. The silicone rubber skin folds and grips the surroundings, providing a passive recovery force that facilitates a peristalsis-like motion to translate the device. More conventional approaches also exist. Desai's group developed SMA-actuated MRI-compatible continuum robots for neurosurgical tasks [93], [94], [95]. A 2018 study combined tendon and SMA-driven methods to build a three-segmented tendon-driven robot for neurosurgery. Each segment housed a nitinol spring that could be temperature-controlled to achieve localized stiffness [96]. Recently, more teams have mimicked the structure of conventional tendon-driven tools with nitinol wire heating [97], and investigated reliability of SMA actuation over repeated loads [98]. Another team took a creative approach to temperature regulation of SMA-actuated MIS tools, using heated or cooled fluid to actuate a surgical gripper [99], [100]. SMA spring-based robotic actuation can be packaged into a small, modular, sterilizable package to build a small, 2 DoF polyamide system as well [101]. Notwithstanding the above applications, SMAs present tremendous potential as actuators for flexible surgical devices robots due to their thin elastic nature and ability to actuate in multiple directions depending on the encoded shape of the alloy. Further, SMAs can be positioned independently of each other, and be individually actuated via fine electrical wire to achieve surgical endpoints. However, limitations remain, such as the potential for damage to surrounding tissue due to heat dissipation, or the barriers in engineering an SMA setup that can match the force output of conventional tendon-driven mechanisms.

A fourth group, which falls arbitrarily between extrinsic and intrinsic actuation, are magnetically actuated continuum robots with on-board magnets. These systems have the benefit of not requiring large on-board motors or pressure chambers to change shape. Further, since any part of these robots can be embedded with actuatable elements, and the source acting on these embedded magnets can be

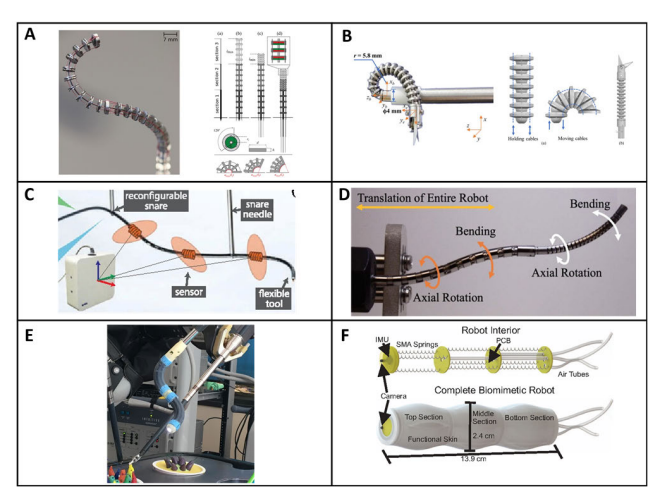


FIGURE 4. Continuum robots are increasingly employing hybrid actuation mechanisms. (A) A hybrid tendon-driven robot with extensible sections mediated by magnetic repulsion [31]. (B) Maxillary sinus surgery robot with rolling joints [40] (©2018 IEEE). (C) CRISP robot employing snares and parallel segments to reach surgical target site and achieve end-goals [46] (©2017 IEEE). [D] Hybrid concentric tube robot that utilizes square notches to actuate the robot in an agonist-antagonist manner [67] (©2021 IEEE). (E) STIFF-FLOP robot for pneumatically actuated endoscopic tasks [102] (F) SMA-actuated soft robot that mimics peristaltic movement for locomotion [92] (©2017 IEEE).

large and versatile (eg. Stereotaxis<sup>©</sup> and Magnetecs<sup>©</sup> catheter manipulation systems), there are functionally infinite DoF in which these machines can be actuated. The efficacy of these systems has been proven in the clinic in the context of catheter-based interventions (discussed further in the Catheter-based Interventions section below). Notwithstanding their value in catheterization, magnetically actuated continuum robots are seeing increased development as teams continue to explore seemingly limitless approaches for actuation modeling (**Figure 3D**). For instance, in a recent study, Lloyd et al. produced soft magnetically actuated continuum manipulators with embedded neodymium-iron-boron microparticles and demonstrated their control in a magnetic field [103]. Another study combined this with shape memory polymer springs and a silicone backbone to create a variable stiffness manipulator [104]. The tool's stiffness can be dynamically adjusted through heating the shape memory polymer springs, allowing for precise control and adaptability in complex anatomical structures. The flexibility of magnetic actuation makes this the third most common actuation approach in hybrid systems (**Figure 3F**).

However, there are inherent limitations to these approaches. For one, accurate and robust actuation of continuum robots requires a powerful and often expensive magnetic setup [105]. Attention must also be paid when choosing materials for such manipulators so as to not interfere with magnetic control or introduce risks into the surgical environment. However, as the role of intraoperative MR imaging increases, and surgeons begin making the transition towards MR-compatible surgeries [106], the avenues for magnetically-guided continuum manipulators for MIS will continue to expand. Another recent study took steps



**TABLE 3.** Brief comparison of actuation principles.

Extrinsic	Type of	Advantages	Disadvantages
or Intrinsic?	Actuation		
Extrinsic Actuation	Tendon- driven and multi- backbone	Relatively lightweight, higher force exertion and payload, scalable, quick response.	Friction along length can damage surrounding tissue, traditional designs cannot achieve extensibility or follow the leader movement, possible hysteresis.
Extrinsic Actuation	Concentric Tube	Small diameter, extensive understanding of kinematics, built-in forward movement, quick response.	Elastic instabilities, limited load capacity, follow the leader movement is difficult to achieve.
Intrinsic Actuation	Pneumatic	Compliant, high-power density for soft actuators, extensible, relatively quick response, stiffening capabilities.	Radial expansion during activation of pressure chambers requires larger diameter, slower response and lower force exertion compared to extrinsically actuated systems.
Intrinsic Actuation	Hydraulic	Compliant, high-power density and force exertion capabilities.	Heavier, slower response time.
Intrinsic Actuation	Shape- memory Alloy	Allows for soft external structure, individually actuatable and independent segments.	Slower response time, hysteresis (depending on the positioning and structure), risk of harmful thermal dissipation.
Intrinsic Actuation	Electroactive Polymer	Can be miniaturized, lower power draw, controllable actuation, lightweight.	Limited load capacity, slower response time.
Other	Magnetic	High degree of motion control, can potentially allow for translation, and navigation of complex routes.	Expensive and large workspace setup, difficult to actuate larger devices with enough power, risk of magnetic interference.

towards this by presenting independently actuated soft magnetic manipulators for bimanual operations. They proposed a method to independently actuate each robot within the same workspace to deliver a camera and optic fiber [107]. A brief comparison of these mechanisms in the context of both conventional MIS and catheter-based interventions has been provided in **Table 3**. Additionally, a brief overview of material classes is provided in **Table 4**.

TABLE 4. Material classifications and use-cases.

Material Class	Examples	Notes
Shape-Memory	Nitinol	Used for their shape-
Alloys (SMAs)		memory and elastic
		properties
Metals	Stainless Steel,	Provide structural
	Aluminum, Titanium,	support and strong
	Copper, Brass,	actuation
	Gallium-based alloys	
Polymers	Polyurethane,	Used for flexibility,
	Polyamide (PA12),	insulation, and
	TPU, PLA, PTFE,	lightweight construction
	PEEK, Silicone	
Elastomers	Ecoflex, Latex	Provide elasticity and
		compliance, often used in
		soft robotics
Magnetic	NdFeB (Neodymium-	Used in magnetic
Materials	iron-boron)	actuation and guidance
3D-Printed	3D-printed resin,	Enable rapid prototyping
Materials	PolyJet-printed plastic	and custom geometries
Composites and	Silicone-NdFeB,	Combine multiple
Hybrids	Steel-Nitinol, Fiber	properties for specialized
	Reinforcement	applications
Natural and	Coffee, Collagen,	Used in granular
Biological	Sucrose	jamming for adaptive
Materials		stiffness

#### IV. VARIABLE STIFFNESS AND SOFT ROBOTICS

Innovators have long looked to nature for inspiration in designing machines, with some of the earliest innovators mimicking bat wings for gliding [108], and others watching plants hook to fur as an inspiration for the invention of Velcro [109]. Of these, an emerging application is that of soft robotics in MIS. As compliant, economical, and patient-specific instruments can significantly increase the safety of surgical interventions, researchers have begun leveraging soft robotic approaches to actuation, such as those discussed above (pneumatic, hydraulic, shape-memory, amongst others). Aside from bio-inspired means of actuation, these robots display another valuable characteristic of soft robots: variable stiffness [110].

From getting to a target site, to performing the operation, compliant flexible manipulators must be able to stabilize their position to A) safely and properly deliver surgical tools, and B) leverage surrounding tissue and organs to get into an ideal position. Various mechanisms have been employed to achieve this variable stiffness, including, but not limited to, multiple-backbone segment stabilization, SMAs, pneumatic, granular and layer jamming, and artificial muscles. Miniaturization, and robust stiffening have become of increased focus. A complete review of the mechanisms of stiffening in flexible and continuum robots is beyond the scope of this systematic review. Readers are pointed to excellent papers that summarize the many mechanisms and their applications here: [111], [112]. This section will instead focus on some common trends and novel mechanisms that may help direct researchers looking towards other solutions.



Continuum robots can be stiffened along their full length, or in segments to achieve specific end goals. Stiffening is yet another characteristic of soft robots that is observed when actuation units are activated [20], [112] (Fig. 5A-D). For example, inflation of a pneumatic chamber can decrease compliance and help secure the device's shape. However, not all stiffening mechanisms reposition a device. Granular and layer jamming are two examples of stiffening mechanisms that instead secure the robot's position [113] (Fig. 5A-B). Granular jamming commonly uses a vacuum, or pressure from neighboring chambers, to force together small particles, such as coffee granules or sucrose [37]. By principle, the higher the pressure difference achieved between external and internal chambers, the stronger the stiffening (Fig. 5B). This can be influenced by the granules used, the structure of the stiffening mechanism, and the materials used to create the chambers [37], [111], [114]. Although granular jamming offers relatively robust stiffening, it has several drawbacks. For one, granular chambers can add significant bulk and weight to the design, without contributing to the maneuverability of the robot. Secondly, modeling the spread of free-moving particles is difficult, with changes in the robot's shape affecting the distribution of the granules. This may lead to unequal stiffening across the length of the granular chamber and thus the manipulator [20], [111]. On the other hand, layer jamming forces together layers of a specifically engineered material instead of granules. This technique leverages frictional interactions between layers and is directly dependent on the type of material used, its frictional coefficients, and the amount of force that can be applied perpendicularly to the layers (Fig. 5A). Although this significantly reduces bulk, it does not offer the same level of stiffening as granular jamming [111], [112].

Since size and stiffening capabilities have been the primary goal of this field, researchers have invented several variants for both granular and layer jamming to address these two bottlenecks. Some approaches again take inspiration from nature. For example, NASA's requirement for a continuum robot for medical interventions in space has driven the development of a "tendril" robot [115]. Various teams have since attempted to innovate solutions to the tendril's shortcomings. With regards to variable stiffening, one team designed a scaly layer jamming system that utilized cable-driven actuation instead of more common pneumatic partners [116] (Fig. 5D.). They employed thin layers of mylar polyester film tightly wrapped around a central spring. Another team took inspiration from both fish and snakes by engineering a helical cable-driven layer jamming mechanism for a STIFF-FLOP module [117]. Both approaches circumvent the traditional limitations of vacuum-based stiffening. Other teams have investigated the efficacy of different modifications to layer jamming. For example, one team produced a prototype soft tendon-driven manipulator with sliding layer variable-stiffening capabilities that utilized the core as an element in the stiffening [118]. The proof-of-concept leveraged a honeycomb central structure to amplify the jamming while

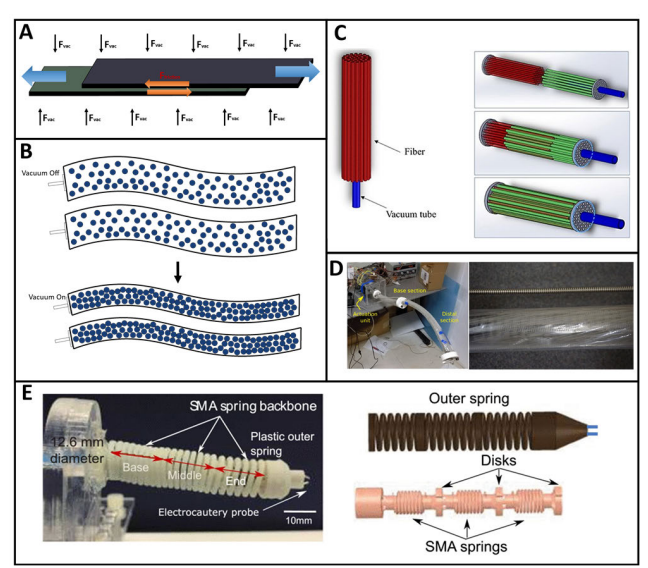


FIGURE 5. Soft continuum robots can stiffen in localized segments to provide a variety of use scenarios. Examples of variable stiffening in continuum robots are highlighted by (A) the principles of layer jamming, (B) granular jamming, and (C) fiber jamming [19]. Examples of variable stiffness continuum robots include designs that use (D) scaly layers [116] (©2015 IEEE), or (E) nitinol tendons and springs to provide segment stiffening [96] (©2018 IEEE).

allowing for reconfiguration of the stiffening region via a sliding layer mechanism. As the vacuum is applied, a friction between the jamming layers and the honeycomb structure provides relatively efficacious jamming [118]. As discussed earlier, recent advancements in jamming for the STIFF-FLOP manipulator have leveraged fiber jamming, which forces together fibers in an intercalated pattern to maximize stiffness in a controllable and predictable manner (**Fig. 5C**) [19], [119], and low-melting-point alloys [75]. This new application of fiber jamming into a soft continuum manipulator brings with it the added benefit of miniaturization and controllability.

These examples demonstrate that these stiffness techniques can be combined with several actuation methods to achieve their end goals. However, variable stiffness is not limited to non-actuator mechanisms, nor is it limited to soft robots. For example, a design employed wire tensioning in the context of cardiac valve delivery [120], and another innovative study reported how coaxial tube-based stiffening can improve the controllability and workspace for steerable needles [121]. They provide flexural stiffness with respect to directed force loads that are mediated by the rotation and translation of the tubes. Another team used SMA-based actuation and segment stiffening in an MRI-guided device designed for neurosurgery (**Fig. 5E**). The group utilized the changing stiffness of nitinol between austenite and martensite states to pull on tendons to bend the continuum robot. The robot itself has three segments supported by nitinol spring backbones, all of which could be similarly stiffened [96].

More recently, electroactive polymers – materials that when electrically stimulated, respond with mechanical motion – have been investigated to actuate continuum robots



for endoscopy applications [122]. Nevertheless, techniques used in soft robots bring an increased measure of safety. The ability to selectively comply with the delicate surrounding environment, and in some designs offer continuous stiffening, can significantly improve the potential of such robots in the surgical environment. As such, soft continuum manipulators may play a considerable role in the development of clinical tools and potential surgical platforms due to their economical, compliant, and self-propelling properties. However, much work remains in force sensing, position, and kinematic modeling.

# V. ROBOTIC CATHETER-BASED INTERVENTIONS

As the push for more minimally invasive procedures continues, endovascular interventions have taken center stage in the treatment of several conditions. These operations leverage long, thin catheters that can navigate the vasculature, guided by x-rays in a process called fluoroscopy, to perform clotbusting [123], endovascular coiling [124], placement of stents for arterial support [125], and drug elution [126] amongst other operations. Most endovascular procedures, however, rely on flexible but passive catheters that require considerable manipulation from the surgeon to navigate the complex anatomy. The surgeon uses rotational movement to direct the catheter to the target site, with no direct control over the steering tip. These devices are thus difficult to navigate with, and the absence of integrated actuation and force feedback presents the risk of damage to surrounding tissue and interventional failure. Additionally, difficulties in navigation and catheter placement increases the procedural timeframe, exposing both the patient and the healthcare team to more radiation [127], [128].

To address these gaps, steerable robotic catheters that are controlled either via tendon-driven, pneumatic, hydraulic, or magnetic-based actuation provide considerable advantages [129], [130]. Various commercialized products have made their way into the clinic, including the Magellan and Sensei robotic catheter systems by Hansen Medical. Other platforms include the CorPath GRX by Corindus, and the Genesis magnetic navigation system under Stereotaxis. A 2018 review provides an excellent introduction to the field and summarizes key design principles [105]. This section will complement and build on this discussion by briefing general actuation principles of robotic catheters, touching on the current state of the art in the clinic, and exploring emerging technologies.

#### A. ACTUATION PRINCIPLES OF ROBOTIC CATHETERS

Unlike the above discussion of robots for MIS, where flexible and continuum tools have the potential for improving operational outcomes, catheter-based interventions have long been made functional by those same characteristics. These devices showcase the role that flexible therapy delivery platforms may play in a robot-driven future for surgery. The main design considerations for catheters include diameter, controllability, DOF, cost, ability to exhibit variable stiffness depending on

the operation, and the biocompatibility and versatility of the materials used to construct these devices.

The most conventional approach utilizes wires to actuate the catheter in an agonist-antagonist manner (Table S1). These are analogous to the cable and multi-backbone rodbased designs discussed above in the design principles of tendon-driven continuum robots. A prime example of this tendon-based actuation in the clinic is Hansen Medical's Sensei Robotic Navigation System. The system can leverage various intracardiac echocardiography, 3D mapping, and fluoroscopy technologies to steer the robotic Artisan® Extend control catheter. To perform electrophysiological procedures, the catheter, which features a central nitinol spine and four tendons for the inner sheath, and separate tendons for the outer sheath, can bend up to 275° in any direction [131]. The distal end offers force sensors that provide tactile feedback to the operator and prevent any advancement once a specific force threshold is breached. The smaller Magellan system has similar working principles and is designed for peripheral vascular procedures. Following suite of this approach, one team showcased the prototyping of an autonomous intramyocardial cell injection catheter that is actuated by four pull wires in an 8Fr package [132], [133]. In addition, the authors also integrated autonomous features to guide the end of the catheter post-calibration. Another team previously also prototyped a tendon-driven robotic catheter for radiofrequency ablation [134]. Jolaei et al. recently proposed a learning-based kinematic model and feedforward position control to validate a control framework for achieving task autonomy in a tendon-driven catheter [135]. These tendon-based systems are relatively straightforward and intuitive, and much work has been done to characterize their kinematics. However, despite their high degree of controllability, they are limited due to similar reasons as those of MIS-focused devices discussed above. Their bulk, and tendency for backlash and hysteresis introduce more barriers in the narrow workspace reserved for interventional procedures.

On the other hand, concentric tube designs offer considerable advantages owing to their small diameters and have been utilized to explore methods for increased safety and force limitation in the delicate environment. Recently, one team was inspired by the wall-following behavior seen in some organisms. To mimic this, they designed an autonomously driven concentric tube catheter system that leverages haptic feedback and surface identification to navigate the anatomy (Fig. 6A). Remarkably, the robot achieved high precision and repeatability to complement the physician's role [136]. This work demonstrated that the understanding and control of concentric tube-actuated robots can effectively be leveraged in an AI-driven package to help achieve operational end-goals. Nonetheless, much work remains in identifying tool-specific and application-specific parameters, as well as overcoming conventional limitations such as pre-defined curvatures, the risk of snapping due to force build-up, and the ability to control the relative rotation of the tubes over long distances in a very delicate, and tortuous environment.



With these fundamentals in mind, another team presented an autonomous navigation paradigm by using simultaneous localization and mapping with a tip-mounted camera to produce safe, autonomous navigation for a concentric tube catheter. This approach also allowed for an approximate follow-the-leader movement [137]. Given these recent advancements, concentric tube-driven catheters can continue to serve as platforms for highly miniaturized tools, although developing a commercially viable and safe systems that can navigate complicated vasculature and comply with the soft anatomy requires much work.

Following suite of the benefits of soft robots, researchers have investigated the potential of hydraulic and pneumatic actuation in robotic catheters. These systems provide considerable advantages due to compliance, quick actuation, and high energy density. They also negate the possibility of electrical discharge in the blood stream by damage to an instrument that uses an electricity-based actuation method. Ikuta et al. developed a hydraulically actuated catheter that has steadily evolved over several iterations. The 3 mm Ø prototype contains multiple bellows actuator segments to navigate more complex vasculature and brings with it the advantage of MR compatibility [138] (Fig. 6B). To help resolve limitations in controllability of the continuum sections, they adopted a "pressure pulse drive" wherein the segments are pumped with waves of pressure to constantly change the base configuration and lead to increased actuation throughout in a relatively controllable manner [139]. Others have focused on the delivery of force feedback and position sensing technology, with a study demonstrating the use of an optic-based sensor to indicate bending angles [138], [140]. More recently, Nguyen et al. developed a hydraulic catheter that could bend 180° with a bending radius of 10mm, making is useful for navigation of small anatomy and interventional tasks such as ablation and clot removal [141]. They also developed a soft catheter tool with hydraulic filament artificial muscles that had controllable extension and flexion purpose built for ablation procedures [142].

Finally, SMAs and electroactive polymers present an exciting area of actuation for robotic catheters. Contrary to Ikuta et al. and Nguyen et al.'s electricity-free designs, SMA-actuated devices leverage the shape-memory effect that is induced by heating an SMA wire (such as nitinol). This allows for highly controllable and fine adjustments, albeit with lower response time and potentially output force. Examples include an SMA-based micro-actuator with a coiled structure that provides over 23° of guidewire bending [143], and an MRI-conditional antagonistic SMA spring actuation-based catheter with a focus on neuro-interventional procedures [144]. Lu et al. designed their nitinol spring actuator to wrap around a guidewire and exhibit semi-autonomous bending that was then tested in vitro [143]. However, given the nature of SMA actuation, and the sensitivity of the vasculature, limitations regarding damage from heat dissipation exist. In the context of MR-compatibility, radiofrequencyinduced heating of conventional metallic guidewires has also limited the scope of such systems [144]. As such, although SMA-actuation provides increased miniaturization, their fundamental barriers must be overcome before they can safely and effectively be combined with advanced guidance modalities and be employed in complex interventional procedures. On the other hand, electroactive polymers provide an alternative solution. These polymers change configuration in a predictable manner when an electric current is applied to them. One team sought to use this approach and created a two-part electroactive catheter with different stiffness characteristics [145]. The high modulus neck is 3cm in length, while the low modulus head is 1cm. Another team developed a "smart" guidewire using an electroactive terpolymer [146] (Fig. 6C). Electroactive polymers may work with lower currents and produce high displacement; however, further challenges exist in reducing the required voltage. Jacquemin et al. recently proposed a polymer to address this and modeled the kinematics of this polymer in the context of MIS [147].

Apart from these electromechanical approaches, wherein the catheter is directly actuated via wires, rods, or other onboard actuation units, some systems take a more distanced approach that is free of such mechanical constraints. Due to their small size, and the ability to precisely actuate a catheter in a narrow environment, magnetic actuation is becoming increasingly feasible. In principle, these systems use embedded magnets to steer the catheter via magnets that surround the interventional bed. Magnetic actuation is generally achieved in two ways. First is the use of electromagnets to generate a variable magnetic field to apply adjustable magnetic force [148]. These magnets require passage of electrical current, which in-turn provides the ability to vary the strength of the magnetic field. However, these systems rely on substantial heat management solutions. On the other hand, permanent magnets cannot readily change their field properties, except by repositioning neighboring magnets [149], [150]. These systems have the advantage of not requiring constant electrical input to activate, although the working environments are limited due to the requirement of specific magnet setups to ensure the magnetic fields are generated in line with the operational requirements. This is because they cannot have a net vector of zero for the generated fields and can pose restrictions to the surgical environment.

Several technologies have taken advantage of this highly miniaturized and controllable approach both in laboratories and in the clinic. Prominent current examples are the Niobe magnetic navigation system [149], [150] and the newer Genesis system, which is both smaller and faster [151]. These systems leverage large permanent magnets that are automatically repositioned throughout the procedure to actuate the catheter. Others include the CGCI system by Magnetecs, which uses 8 fixed electromagnets to articulate the catheter [148].

Given their clinical potential, several teams have pioneered developments to overcome the traditional barriers



of magnetically actuated catheter systems and to further our understanding of their articulation and versatility. For example, a group at MIT created a ferromagnetically actuated soft polymer-based catheter prototype that is embedded with neodymium-iron-boron alloy microparticles and actuated by a manually positioned permanent magnet [152]. This continuum device was navigated through a complex cerebrovascular phantom setup to demonstrate the accuracy and high level of articulation that is achievable with such forms of magnetic actuation (Fig. 6D). These tools can further provide interventional options to hard-to-reach targets, as demonstrated by the routing of an optical fiber through the device to demonstrate the principle of laser delivery [152]. Other solutions such shown by Lloyd et al. feature discrete magnetized segments that would collectively be actuated by surrounding magnets [103]. This device was made with Ecoflex 00-30 elastomer embedded with neodymium-iron-boron microparticles in a 1:1 weight ratio. Another team produced a variable stiffness magnetic robotic catheter [153], [154]. Unlike conventional catheters, these individually stiffened segments allow the robot to achieve complex shapes which can better help it navigate tortuous environments. The variable stiffness segments are based on a low melting point alloy which allows precise control of the robot. Another team developed a 2mm diameter magnetic catheter with two magnets and drill tip and demonstrated unclogging of a blot clot in vitro [155] while others used embedded electromagnetic coils to magnetically guide and actuate their catheter [156]. Another study proposed an electromagnetically-powered propulsion and control model of a steerable needle [157], while Jung et al. optimized a steering approach by using a magnetic setup specific for their catheter's path [158].

As many teams have worked on improving magnetic actuator control for endovascular procedures over the past two decades, others have attempted to overcome limitations in the magnets that control the catheters as well. For example, one team attempted to overcome a limitation of permanent magnet setups that prevent a field gradient of zero. Instead of inducing large translocations of permanent magnets, they used an array of rotatable permanent magnets that enabled 5 DOF control of a microrobot [159]. Other teams proposed a hybrid actuation and control method to develop variable stiffness catheters by incorporating magnetic actuation with a shape memory polymer [160], [161]. Active heating and cooling helped achieve variable stiffness and higher dexterity. Another recent study describes a millimeter-scale magnetic steering continuum robot for transluminal procedures. This robot can navigate complex pathways by alternating between solid and liquid states and using programmable magnetic fields, allowing it to move safely and morph into functional tools or sensors in larger anatomical spaces [162].

Despite their tremendous clinical potential and increased usage, magnetic catheter actuation systems have limitations. For example, these systems commonly require large, expensive setups that also lack portability. The need for additional operating room standards such as magnetic-compatible apparatus and shielding also restrict the accessibility of such systems. Future innovations will attempt to address these, and work on increasing controllability of interventional devices, studying the efficacy of various embedded microparticles and their distribution, more acute actuator sources, and the investigation of creating powerful, tunable sources of actuation from permanent magnets that employ a full range of magnetic gradients.

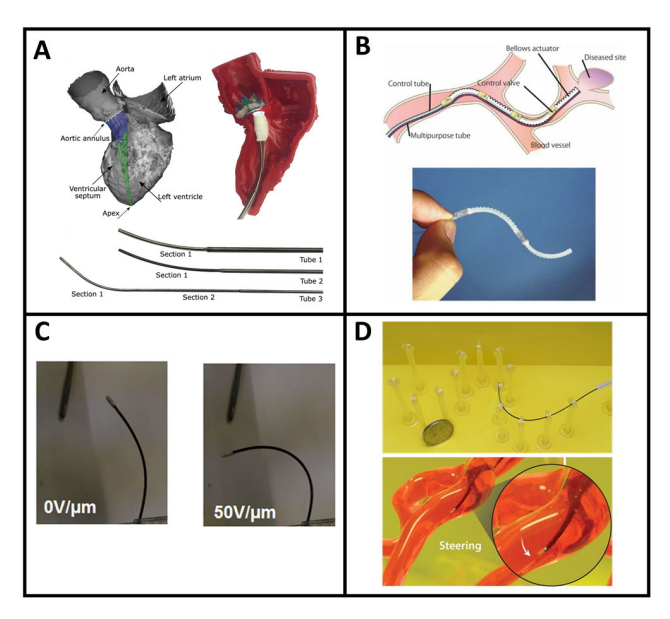


FIGURE 6. Robotic and steerable catheters employ several actuation mechanisms, each with their own benefits and drawbacks.

(A) Autonomous concentric tube robot for intracardiac navigation based on haptic vision feedback [136]. (B) Hydraulically actuated soft catheter with optical sensors for bending [138] (©2016 IEEE). (C) Smart guidewire made from electrostrictive polymer that is activated with the input of current [146]. (D) Neodymium-iron-boron microparticle-embedded ferromagnetic catheter that is actuated by the localization of a permanent magnet and delivers an optic fiber to demonstrate the ability to deliver a laser [152].

# VI. FORCE FEEDBACK AND POSITION TRACKING

For decades, surgeons have grappled with the question of how to provide minimally invasive interventions, whilst being fully aware of the internal anatomy within an operation. Traditionally, surgical workflow would have to be stopped, the patient transported for imaging, and then the operation continued based on this feedback. The introduction of intraoperative imaging significantly improved this and provided physicians with up-to-date images with which to navigate and continually plan their operation [106], [163], [164]. As the scope of interventional robotics increases [165], and the potential of continuum robots in MIS becomes more prominent, so too does the need for advanced position and force feedback. Here, we summarize the major solutions teams have utilized for continuum robots and touch on emerging approaches. We focus on recent work while adding to a



previous in-depth survey by Shi et al. [166] on shape sensing for continuum robots in MIS, and Ramadani et. al. [167] on catheter tracking methods.

Beginning with traditional endovascular interventions, one common mode of tracking catheters is by fluoroscopy, which uses continuous x-ray to observe movements within the anatomy. Both manual, and now robotic catheter systems are commonly made compatible with x-ray-based imaging and tracking processes, either by nature of a part of surgical tool, or by a contrast dye [168], [169]. This imaging technique has allowed physicians to perform interventional procedures in a relatively high-resolution and economical manner without the need for large cuts and invasive operations. However, fluoroscopy comes at the cost of relatively large amounts of radiation exposure which can potentially be damaging to long term patient health [170]. Over the years, various teams have investigated how to improve 3D reconstruction and kinematics whilst also limiting radiation exposure. For example, one team leveraged probabilistic priors and numeric optimization with kinematic models for a concentric tube robot to present a shape estimation model. This approach used a set of fluoroscopic images to predict the position of the deformable robot over time with a substantial degree of accuracy [171]. Another study employed image feedback and a Cosserat rod model to estimate forces in a microscale tendon-driven guidewire robot, achieving an average RMSE of 0.46 mm in shape predictions for notched nitinol tubes [172]. Another study presented a tracking model using monoplane fluoroscopy that compensated for 3D breathing motion for a radiofrequency ablation catheter [173]. The approach was particularly effective in minimizing drift and directly provided correction for 3D translational motion. To increase accuracy, others have instead opted to investigate biplane fluoroscopic imaging to track instruments. For example, Wagner presented an algorithm that provides 3D reconstruction of deformational devices in the vasculature [174]. It is, however, important to note that although more powerful, biplane approaches increase radiation exposure [175], [176]. Overall, model-based and region segmentation approaches provide powerful tools for tracking catheters [177] and guidewires [178] via fluoroscopic means. On the other hand, ultrasound serves as a safer and more economical, albeit lower resolution solution for catheters [179]. For example, one team used 2D ultrasound to track a flexible needle in 3D [180] and another team used 2D ultrasound images and kinematic information for tip position estimation of a concentric tube robot [181].

Due to concerns about x-ray radiation and poor soft tissue visibility, the use of MRI as an alternative tracking solution has been increasingly explored since its first clinical use in cardiac catheterization [182]. However, interventional MR-guided catheterization procedures face a bottleneck due to a lack of guidewires and other interventional instruments that are MR-safe and provide both exceptional control and force output. Nonetheless, researchers have innovated

solutions by testing various materials such as Kevlar with short nitinol modules under both active and passive MRI visualization [183]. Thus, demonstrating the feasibility of glass-fiber epoxy-based guidewires in porcine models under the guidance of a 3T MRI [184], and a synchrony of previous advancements by using an MR-compatible non-metallic Kevlar-braided guidewire to deliver non-metallic stent scaffolds [185], amongst other investigations [186], [187], [188]. Another team took on the challenge of circumventing traditional MR-incompatibility of metallic guidewires [189], [190]. Basar et al. constructed electrically insulated nitinol guidewire segments that were 0.25λ of radiofrequency transmission at 1.5T, and demonstrated that they were MRsafe [189]. This was built on by constructing a stainless steel-braided catheter with a more continuous electrical flow, which was instead interrupted in 10 cm intervals [190] (Fig. 7A). A primary focus of the field remains the development of robust, actuatable, MR-compatible guidewires with exceptional visibility under both active and passive imaging that can synergize with advancements in MR and hybrid electrocardiographic imagery. For an in-depth review of this field, readers are pointed to excellent articles that evaluate the strengths and weaknesses of different MR visualization approaches, materials used in MR-compatible guidewire design, and their applications [191], [192], [193].

Electromagnetic (EM) tracking sensors are another widely used technology that can provide real-time tracking of small objects without any line-of-sight limitations. Due to their small size, electromagnetic sensors can be embedded onto robots and their positions used to estimate the shape of the device within an electromagnetic field. Various examples have been demonstrated in both catheters and conventional MIS robots. For example, Dupourqué et al. introduced an electromagnetically assisted three-section robotic catheter with follow-the-leader movement for transbronchial biopsies [194]. An SMA-actuated robot for MRI-guided neurosurgery used an EndoScout sensor (Robin Medical, Inc., Baltimore, MD, USA) to track the robot within a magnetic field [96], while another team leveraged the Aurora System (Northern Digital Inc., Waterloo, Canada) to track the tip of their fetoscopic robot [195]. Another team used it to track their CRISP robot [46]. Song et al. embedded multiple sensors along the length of their robot to track the shape of their device in realtime [196], while a classic example of the highly articulated probe used only one sensor, located at its tip, due to its ability to exhibit follow-the-leader movement [197].

Electromagnetic tracking sensors benefit from coupling with kinematic modeling to predict robot shape and position in real-time. For example, shape reconstruction in Song et al.'s multi-section robot could be achieved by fitting multiple quadratic Bézier curves based on the positional data provided by the electromagnetic sensors. This helped them achieve a mean position error of 1.7 mm [196]. The integration of electromagnetic sensors with modeling in CRISP robots was explored to investigate a tracking paradigm for



such robots [46]. On the other hand, Back et al. sought to improve catheter guiding without being fixed to kinematic modeling, and provided a model-free tension based control algorithm for tracking [198]. Song et. al. proposed an extended Kalman filter (EKF) algorithm for tracking multi-arm continuum robots by integrating the poses calculated from both the kinematic model and the magnetic field model, enabling the achievement of multi-target positioning in surgical navigation [199]. Despite their widespread use in research, inherent limitations exist, as magnetically guided devices are susceptible to magnetic interference and require supporting setups to record the position and shape of the robot.

While fluoroscopic, magnetic, and visual (the use of cameras to view and estimate position) approaches have traditionally dominated, another promising approach is that of fiber optic sensors. Most recently, fiber Bragg gratings (FBG) have seen increased use as a solution for shape sensing in various MIS continuum robot applications. These sensors are integrated into single fibers, differentiated by a change in the refractive index of the fiber, and are resistant to magnetic interference [200]. When a strain is applied, the wavelength of light that is reflected changes accordingly. A multiplexed system of sensors can thus provide valuable shape reconstruction information to operators, although single-core setups are prone to errors due to multi-reflections [201]. Multicore systems, which feature multiple sensors per fiber, are more complex, but offer solutions via sensor redundancy and exceptional miniaturization. For example, multicore fibers have recently been used for shape reconstruction of small sections of catheters with a 118 mm sensing length [202]. The same group later used Bishop frame equations with the curvature interpreted from their FBG sensors to reconstruct the robotic pose [203]. Another team used their multicore sensor setup to optimize FBG shape sensing to a considerable degree of accuracy for their endovascular catheter over a 38 cm sensing length [204]. Other creative approaches have been leveraged to optimize shape sensing in different environments. For example, Chitalia et al. placed their fiber within a nitinol tube with a shifted neutral axis to provide repeatable compressive strain for curvature estimation and shape sensing (Fig. 7B). They employed a Kalman filter based observer to validate the efficacy of their sensing technique in the context of large deflections in their mesoscale robot [205]. A more classical example explored variations to traditional FBG substrates by testing polymer tubes to provide a potentially more economical solution, but with less rigidity. They used three-part FBG units mounted sequentially to their braided polymer tube to test the strain transfer between the polymer tube and glass fiber [206]. The SMA-actuated MINIR-II robot by Desai's group also featured a modular PDMS-encased FBG sensor [207]. Contrary to the traditional notion of continuum robots being limited to softer and more delicate tasks, researchers took advantage of the flexible technology for the insertion and fixation of bone fractures while employing continuum robot-deployed curved drilling [208], [209], [210], [211]. In a recent study, FBG sensors are used and provided adequate precision for shape reconstruction of a continuum dexterous manipulator undergoing large deflections in the presence of external obstacles [212]. Dai et. al. proposed a novel friction measuring method using FBG sensors—enabling full friction distribution measurement and improving static model accuracy particularly with inconsistent friction directions [213]. Yi et. al. presented a real-time shape estimation method for a hyper-redundant manipulator with embedded coiled fiber sensors which are flexible, compact, and cost- effective. The method guarantees accurate shape recognition under external loads [214]. The "orthosnake" uses six FBG nodes compiled into two sensor arrays placed inside nitinol wires to provide feedback about the curvature of the robot (Fig. 7C). Finally, given the inherent benefits of soft robots in MIS applications and their scope as an emerging field, optic fiber arrays have also been used to predict real-time shape detection and large deformational tracking in a bellows-shaped soft manipulator [215]. The proposed approach is based on parallel dual-fiber FBG arrays that compensate for temperature and axial force effects on the calculated curvature and demonstrate the versatility of optic-based sensors in shape sensing of soft robots. In recent years, deep learning approaches have been employed for shape sensing in continuum robots using FBG sensors [216], [217], [218]. Schwarz et. al. introduced a novel method that uses a deep neural network to estimate CDM shapes from FBG sensor data and incorporates uncertainty estimation to improve reliability. Their approach enhanced shape prediction accuracy while addressing uncertainties in neural network predictions, and validated this through bending and position estimation experiments [219].

FBGs also have the added benefit of force sensing, which can make the difference between a failed or successful operation. Without adequate force feedback, there is an increased risk of harming the patient. Work is underway to provide increased insight and to leverage such tools for different applications. For example embedded force sensors have used environment contacts to provide valuable feedback for catheters and can estimate the contact forces throughout the robot's length [220], while other approaches such as the piezoresistive sensor in the robotic hand of the CathROB provide an indication of force feedback to alert the operator of high force output and to provide an automatic safety stop when a certain force threshold is breached [221]. Others have pointed to the unique advantage of soft robots given their inherent force sensing applications [86]. Force sensing by FBG sensors is a rapidly expanding field in continuum robots for MIS and interventional procedures. For example, Cheng and Law used three FBG wires for their force sensor that allowed them to detect the relative position of the catheter to the heart wall (Fig. 7D). This informed the autonomous robot whether the heart was contracting or relaxed [132]. Gao et al. used FBG sensors to estimate



robotic body contact and presented a mechanical model to simulate this [222]. Other teams devised creative solutions to simultaneously measure curvature, torsion, and force by helically embedding the FBG sensors into the robotic shaft [223], or using a well-positioned sensor array to measure forces in tumor localization tasks [224]. Both Rigid Link approximation and Cosserat rod theory models have been tested and compared for their accuracy in the context of FBG force sensing [225]. Further details about sensing technologies in continuum robots are described in a recent review [226]. Although further work remains in increasing sensor accuracy, improving temperature compensation and shape reconstruction in a variety of application pipelines, FBGs offer a unique avenue to miniaturize and track not only the robots, but also operational endpoints.

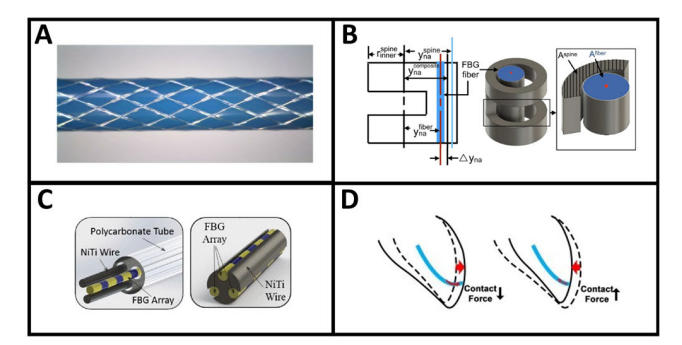


FIGURE 7. Various tracking and force sensing modalities complement the capabilities of continuum robots in different surgical interventions. (A) Insulated stainless steel wire braiding interrupted in 10 cm segments to achieve for MR-safe metallic guidewires [190]. (B) FBG fiber in a shifted neutral axis notched nitinol tube for compressional strain [205] (©2020 IEEE). (C) Three-node FBG array setup within nitinol tube to provide feedback on the ortho-snake [211] (©2019 IEEE). (D) FBG-based force feedback for autonomous robot in the heart [132].

Looking to the future, autonomous control and tracking of robot position will continue to gain interest and feasibility. As a result, vision-based tracking methods have emerged, promising real-time, non-invasive position tracking without the need for additional sensors. Wang et al. proposed a color-enhanced random forest model for tracking the position of tools in MIS [227]. This method leverages a combination of segmentation and kinematic modeling to estimate the position of surgical tools in endoscopic images. The integration of 3D vision cameras, marked surgical tools for reference point tracking, and better force estimation markers based on tissue data collected with MIS cameras may form the basis for a comprehensive, live 3D model of the surgical space. With sufficient data, AI-driven position and force estimation may demonstrate the potential of vision-based tracking to enhance the adaptability and miniaturization of MIS tools.

# VII. MODELING AND CONTROL

Unlike conventional robot manipulators that are characterized by rigid links and have standard methods for kinematic and dynamic modeling [228] and control [229], it is difficult to establish a standard for modeling continuum robots due to their custom designs and structural complexity. This is particularly complex in the context of robot-assisted MIS [230], [231]. To address these limitations, several works have been presented by researchers in modeling [232] and control [233] of continuum robots over the last few years.

Modeling continuum robots using analytical methodologies typically consists of two main frameworks, namely, kinematics and mechanics [14], [16]. The kinematic framework describes the shape (position and orientation) of the robot by a set of configuration coordinates. The mechanics framework incorporates principles of mechanics, constitutive equations, virtual work, etc., to represent the effects of actuation and external loads (forces/torque) on the configuration and motion of the robot.

# **VIII. KINEMATICS**

Analytical models have been proposed based on kinematics frameworks. For example, researchers modeled the kinematics of continuum robots by approximating their structure with discrete rigid links [234], [235], [236], which is a common method for modeling conventional rigid-linked robot manipulators. This approach models the robot with a set of rigid links that are connected with conventional revolute, universal, or spherical joints. The kinematics formulation is described by a sequence of homogeneous transformations derived from the standard Denavit-Hartenberg (D-H) parameters table. The discrete rigid link model is appropriate for conventional manipulators with discrete rigid structures, yet it can represent continuous elastic structures with good approximation. The discrete approach is also employed in estimating the shape and external loads of a continuum manipulator, utilizing pseudo-rigid body (PRB) models. An array of electromagnetic coils is utilized to model and generate external loads, enabling the actuation of a magnetically driven continuum robot. The robot's continuous shape is approximated through the connection of four discrete rigid links by three 2-DoF joints [237] (Fig. 8A). Huang et al. introduced a MCR with two DoF and developed a deformation estimation algorithm based on the PRB model, which allowed better control. Integrated with mechanical systems and Jacobian-based control, the MCR achieved precise tip trajectory tracking and obstacle avoidance, making it a promising approach for interventional procedures [238].

Unlike discrete rigid links approaches, piecewise constant-curvature kinematic models comprise a finite number of curvilinear sections (**Fig. 8B**). The typical assumption is that each of these controllable sections maintains a constant curvature with respect to the arc length variable, s. Successive pairs of these sections are then tangentially aligned, creating a continuous tortuous shape to represent the geometry of continuum robots [239]. Camarillo et. al. proposed a constant curvature model based on circular bending and axial deflection. This model accounts for the distribution of forces between tendons and the manipulator's structure, establishing



a method to map tendon displacement to manipulator configurations [240].

Assuming, piecewise constant curvature (PCC), Peng et. al. introduced a shape estimation method using multi-IMU fusion for a tendon-driven continuum robotic manipulator which demonstrated strong 3D-movement accuracy [241], while Sayadi et. al. modeled a steerable ablation catheter with a finite number of constant curvature arcs [242]. Further details about constant curvature models can be found in a review by Webster and Jones [52].

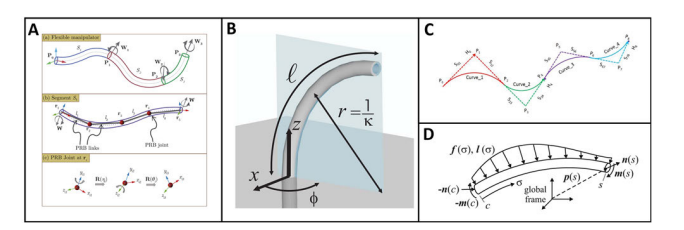


FIGURE 8. Schematics of different kinematics modeling approaches. (A) The pseudo-rigid body modeling approach involves substituting the continuum robot with a sequence of discrete rigid links, each link having a length li  $\in$  R+ connected by joints at positions  $ri \in$  R3. Each joint has two intrinsic rotations: the first rotation  $R(\eta i) \in$  SO3 is about the y-axis by an angle  $(\eta i)$ , succeeded by another rotation  $R(\theta i) \in$  SO3 about the z-axis by an angle  $(\theta i)$  [237]. (B) The constant curvature modeling approach describes the continuum section with a circular arc with configuration variables such as arc length (I), plane  $(\phi)$ , and curvature  $(\kappa)$  [52]. (C) Parametric curve-based methods (Bézier curves) [196] (©2015 IEEE). (D) A typical free body diagram used in the Cosserat rod theory for an arbitrary segment of a beam for the arc variable changing from c to s and subject to internal forces and torques n(.) and m(.), respectively. The external force and moment distributions are respectively represented by  $f(\sigma)$  and  $I(\sigma)$  [243].

While constant-curvature kinematic models provide superior shape approximation in many continuum robots compared to discrete rigid link approaches, the assumption that the curvature of each actuatable section remains constant at every time instant with respect to the arc length variable is a simplification of the actual physical phenomenon. Particularly, when a single actuatable section is relatively long, points at different locations with distinct arc length variables, 's,' can exhibit different curvatures at the same time. Thus, the constant-curvature assumption may not align well with reality. Consequently, there is a push to develop variable-curvature kinematic models that account for curvature variations with respect to s. To this end, researchers developed different types of variable-curvature models to represent continuum robot kinematics. For example, Euler spirals, also known as Clothoids or Cornu spirals, in which the curvature is directly proportional to the arc length s, are used to approximate the continuum robot's shape [244]. It has been shown that Euler-based models could generate a faster response in curve approximation while providing sufficient accuracy in the presence of external tip forces [245]. Zhang et al. proposed a new design for a tendon-driven quasi-continuum robot that uses a non-constant subsegment stiffness structure. They integrated rigid-flexible coupling to improve load handling without sacrificing flexibility. Using the Newton-Euler formula, they proposed a modeling

technique that transitions from static to kinematic analysis, employing screw theory for kinematics and addressing tension losses due to friction [246]. Jiajia et al. introduced a new inverse kinematics method using Kepler ovals for both single- and multi-segment continuum robots. Since the assumption of linearly increasing curvature does not suit all continuum robot designs, the study explores alternative models that account for variable curvature to for broader applicability [247]. To consider the effects of torsion on kinematics, researchers employed exponential coordinates based on Lie group theory to represent the spatial configuration of continuum robots [248], [249].

In recent years, several kinematics models for shape reconstruction of continuum and soft robots have been developed based on parametric curves such as Bézier curves [250], [251]. A Bézier curve of degree n can be defined as,

$$C(q) = \sum_{i=0}^{n} P_i B_i^n(q), \quad 0 \le q \le 1$$
 (1)

where C(q) is a vector-values function of a normalized independent value q,  $P_0$ ,  $P_n$ , are the beginning and ending points of the curve,  $P_i \in R^d$  are the control points, and the basis functions,  $B_i^n(q)$ , are the Bernstein polynomials of degree n defined as,

$$B_i^n(q) = \frac{n!}{i! (n-i)!} q^i (1-q)^{n-i}, \quad i = 1, \dots, n$$
 (2)

Quadratic and cubic Bézier curve methods have been used for real-time shape reconstruction with electromagnetic (EM) tracking sensors [196] (**Fig. 8C**). In another study, a kinematics model is proposed using a combination of Biarc and Bézier Curves [252]. Yuan et. al. used a cubic Bézier curve method with an EM sensor in a kinematics-static model for external force estimation [253].

Non-uniform rational B-splines (NURBS) present another commonly utilized parametric curve model in computer-aided design and manufacturing (CAD/CAM) for describing curved lines and surfaces [254]. Similar to the Bézier curves, the B-spline curve can be defined as follows,

$$C(q) = \sum_{i=0}^{n} P_{i} N_{i}^{k}(q), \quad 0 \le q \le q_{max}$$
 (3)

in which  $P_i$ 's are control points (also known as deBoor points) and  $N_i^k(q)$  is the *i*-th B-spline basis function of degree k, which is represented by a recursive equation as

$$N_{i}^{k}(q) = \frac{q - q_{i}}{q_{i+k} - q_{i}} N_{i}^{k-1}(q) + \frac{q_{i+k+1} - q}{q_{i+k+1} - q_{i+1}} N_{i+1}^{k-1}(q)$$

$$N_{i}^{0}(q) = \begin{cases} 1 & \text{if} \quad q_{i} \leq q \leq q_{i+1} \\ 0 & \text{else} \end{cases}$$
(4)

Spline-based methods are also used by researchers for modeling continuum trunk [255], endovascular catheterization [256], and soft robots [257], [258]. Compared to Bézier curves, B-splines offer increased degrees of freedom and



enhanced flexibility. This is attributed to their capacity for localized curve shape control and the independence of the curve's degree to the number of control points. Despite these advantages, B-splines are constructed from multiple polynomials connected at knot points, introducing complexity and potentially reducing stability. This complexity can pose challenges, particularly when applied to the shape reconstruction of continuum robots.

Pythagorean hodograph (PH) curves (260) is another method that is used to resolve the complexity and computational instability problem of B-splines by introducing a closed-form solution for curved shapes [260]. For example, Singh et. al. utilized a PH-based modeling approach for shape reconstruction of the Compact Bionic Handling Arm (CBHA) robot [261]. In another study, a kinematics model based on a combination of Bézier Curve and Pythagorean Hodograph (PH) is proposed for shape reconstruction of a continuum robot using IMU and vision sensors [262]. Mbakop et. al. used a combination of a reduced order PH curve and a Gauss-Lobatto quadrature for modeling and control soft-continuum manipulators [263].

#### IX. MECHANICS AND DYNAMICS

Many model-based control approaches for continuum robots focus solely on kinematics, neglecting mechanical and dynamic factors such as tendon tension, internal friction, and reaction forces. While incorporating these factors leads to more complex models and higher computation times, their influence on the robot's shape is significant. Recently, methods have been introduced to account for these mechanical effects in control frameworks. In this section, we provide a brief overview of two commonly used mechanics models for continuum robots: Energy-based formulations and Cosserat rod theory.

Energy-based approaches are used to formulate the shape of continuum robots. For example, Euler-Lagrange equations derive the dynamics of continuum robots by establishing a Lagrangian function. This function is computed considering the kinetic energy arising from the robot's motion, and the potential energy, which results from the effects of elasticity and gravity on continuum robots. The Lagrangian function was formulated for either lumped [264] or distributed [265] mass model assumption. Del Giudice et. al. developed an energy minimization approach using Lagrange equations with internal kinematic constraints to predict the turning points of a multi-backbone continuum robot [266]. Yang et. al. developed a kinematic and analytical stiffness model for dynamic behaviors using Euler-Lagrange equations [267]. A similar approach is employed for wrench estimation [268]. One challenge in dynamic modeling of cable-driven continuum robots with NiTi wires is the stress-strain hysteresis effects of NiTi alloy, due to their viscoelastic properties. To resolve this, one group proposed a fractional-order Euler-Lagrange equation for improved dynamic modeling [269].

Another modeling approach is based on continuum mechanics theory and is characterized by different models for material properties such as strain theory [270], [271] for elastic material and hyper-viscoelastic models (e.g. nonlinear Kelvin-Voigt model [272]) for hyper-elastic materials. The mechanics framework can be represented by infinite-dimensional configuration space models such as Cosserat rod theory [273] or beam theory [274].

The Cosserat rod theory has been widely used in recent years for modeling both kinematics and mechanics/dynamics of different continuum robots including, tendon-driven [232], [275], soft robots [276], [277], concentric/eccentric tube robots [278], [279], to name a few. Wang et. al. presented a Cosserat rod-based model for a variable stiffness granular-jamming-based soft continuum robot. This robot featured a growing spine and its movement was accurately modeled using this Cosserat rod model [280]. Hanza and Ghafarirad introduced an inhomogeneous Cosserat rod theory to model the shift of the neutral axis in a 3-tube soft continuum robot, and experimentally validated their approach [281].

Kolahi et. al. applied Cosserat theory to model the control and movement of continuum robots with permanent magnets or ferromagnets under magnetic fields, which may help improve tracking and movement modeling during surgical interventions with such devices [282].

In Cosserat rod theory, the configuration of a thin rod is determined by employing a continuous homogeneous transformation with respect to the robot's arc length variable, s. The shape of the robot is represented using a position vector  $P(s,t) \in R^3$  and a rotation matrix  $R(s,t) \in SO(3)$ . The rotation matrix is based on a set of orthogonal directors  $(d_x,d_y,d_z)$  of the locally attached frame, where  $d_x$  and  $d_y$  are in the cross-section plane and  $d_z$  is orthogonal to the cross-section plane  $(d_z = d_x \times d_y)$ . The differential kinematic equations alongside the arc length variable, s, can be written as

$$\frac{\partial P}{\partial s} = P_s = Rv \tag{5}$$

$$\frac{\partial R}{\partial s} = R_s = R\hat{\mathbf{u}} \tag{6}$$

where the vector  $u = [u_x, u_y, u_z]^T \in R^3$  represents the rates of angular changes about the local axes of R(s, t). In other words,  $u_x$  and  $u_y$  describe the rate of bending and  $u_z$  describes the rate of twisting. The vector  $v = [v_x, v_y, v_z]^T$  T includes the rates of linear changes. Specifically,  $v_x$  and  $v_y$  describe the rate of shear, and  $v_z$  describes the rate of extension. A special case of the Cosserat rod theory where no transverse shears and axial strains are considered is called the Kirchhoff rod model [283]. The operator  $\hat{(}): R^3 \to so(3)$  represents the mapping operator from a three-dimensional vector space to its crossproduct skew-symmetric matrix in the special orthogonal Lie algebra, so(3), and is formulated as

$$\hat{\mathbf{u}} = \begin{bmatrix} 0 & -u_z & u_y \\ u_z & 0 & -u_x \\ -u_y & u_x & 0 \end{bmatrix}$$
 (7)



In addition to the feasible assumption of quasi-static motion, which is suitable for the typically low-speed movement of many medical continuum robots, the dynamic motion of these robots is also explored by considering the temporal rate of changes in the geometry of the rods. This involves studying the dynamic aspects that account for variations in the shape and configuration of the continuum robots over time and is represented as

$$\frac{\partial P}{\partial t} = P_t = Rq \tag{8}$$

$$\frac{\partial R}{\partial t} = R_t = R\hat{w} \tag{9}$$

where q and w are the temporal linear and angular rate of change.

The free body diagram for any arbitrary segment of the beam is illustrated in **Fig. 8D**, in which n(s) and m(s) stand for the internal force and moment vectors in global coordinate, and  $f(\sigma)$  and  $l(\sigma)$  represent the external force and moment distributions per unit length of the arc parameter s. By establishing equilibrium force and moment equations and computing their derivatives with respect to s, the dynamic Cosserat equations in the global coordinate can be expressed as follows [243]:

$$R\left(\frac{\partial n(s)}{\partial s} + f(s)\right) = \rho A(s)P_{tt} \qquad (10)$$

$$R\left(\frac{\partial m(s)}{\partial s} + \frac{\partial P(s)}{\partial s} \times n(s) + l(s)\right) = \rho J \frac{\partial R_w}{\partial t}$$
(11)

in which  $\rho$  represents the mass density, A(s) is the cross-section area, and J is the second moment of the cross-section area matrix. The time derivative terms are set to zero for the quasi-static motion assumption [284].

The kinematic variables in the equations (5)-(9) can be related to the internal forces and moments in the dynamic equations (10) and (11) using the following mechanical constitutive relations

$$n(s) = R(s)K_{se}(s) (v(s) - v^*(s))$$
(12)

$$m(s) = R(s)K_{ht}(s) (u(s) - u^*(s))$$
 (13)

$$K_{se}(s) = diag(GA(s), GA(s), EA(s))$$
 (14)

$$(s) = diag(EI_{xx}(s), EI_{yy}(s), EI_{zz}(s))$$
 (15)

where  $K_{se}$  and  $K_{bt}$  denote the stiffness matrices, with the former corresponding to shear and extension, and the latter relating to bending and torsion. A(s) represents the cross-section area, E is Young's modulus, G is the shear modulus,  $I_{xx}$  and  $I_{yy}$  are the second moments of cross-section area about the principal bending axes, and  $I_{zz} = I_{xx} + I_{yy}$  is the polar moment of cross-section area about the torsion axis, which is normal to the cross-section at the centroid.

The integration of these kinematics, dynamics, and constitutive equations results in a system of nonlinear partial differential equations. For example, Till et al. employed an implicit method for discretizing time derivatives, converting the partial differential equations into a boundary value

problem with respect to arc length at each timestep [285]. Abu Alqumsan et al. employed the Generalized- $\alpha$  method to enable computationally effective modeling on a continuum robot [243]. While Cosserat rod theory often relies on linear constitutive models from beam theory, it can also incorporate more complex material behaviors, enabling broader application in robot modeling. Several other researchers have also studied the effects of grasping forces [286], cable friction forces [287], [288] and external loads [289], [290], [291].

In addition to energy-based methods and Cosserat rod theory, other approaches to dynamic modeling include multi-flexible body dynamic modeling, which may be more applicable models for soft robots [292]. Machine learning (deep learning) methods have also been widely used in recent years to model kinematics and dynamics of continuum and soft robots. Discussion about the details of such methods is beyond the scope of this work and interested readers are directed to recent reviews about the application of different machine learning-based approaches in modeling [293], [294] and control [295], [296] of continuum and soft robots [276].

## X. DISCUSSION AND FUTURE DIRECTIONS

Much progress has been made over the last decade in understanding continuum robots in the context of MIS. Several frontiers have emerged as physicians, engineers, and mathematicians work together to push the boundaries of surgery. In this review, we attempted to provide a streamlined summary of some of these avenues by amalgamating studies that emerged in a systematic search over four databases. We also highlighted novel developments in conventional MIS, soft robotics, and robotic interventional surgeries. We covered actuation mechanisms, robotic configuration, tracking, force feedback, and provide commentary comparing pertinent advancements. Due to the nature of the topics covered, wherein conventions for comparing such tools are not thoroughly established, we followed Runciman et al.'s approach for reporting key design characteristics [20].

From the studies highlighted in this review, we see that progress has been made in addressing key challenges identified by [14] and [191]. Notably, the increased emergence of hybrid actuation, magnetic actuation, the combination of imaging modalities with less conventional modes of catheter control, as well as the increasing role of soft robots seem to be emerging as potential solutions to current limitations. For the first time, scientists have begun to integrate automated navigation of catheters based on machine-learning approaches that are inspired by nature. Given this, we acknowledge that significant barriers continue to persist. For one, modeling the structure, deformation, and compliance of soft robots with non-uniform shapes remains complex, and the delivery of tools via variably stiffened soft platforms requires more robust and miniaturized solutions. In the broader context, integrating real-time 3D reconstruction of continuum robots into commercial systems still has considerable potential.



While we envision that highly articulated continuum robots may one day bridge the gap between current robotic platforms and achieving consistently better surgical timelines and patient outcomes, several focus areas are crucial for sustained growth. For one, given that researchers can now successfully model autonomous movement for some actuation models, innovating solutions that can repeatedly and consistently enable follow-the-leader movement to navigate the anatomy - both forward, and backward - would significantly add to the repertoire of such systems. Secondly, given that soft tissue is compliant, dynamic, and at the risk of damage from hard tools, developing safe and reliable soft robotic chassis would have the potential to substantially reduce the risk of internal trauma. In addition to providing safe robot-tissue interaction, leveraging the inherent force sensing abilities of soft systems may provide added situational awareness and overall confidence in the procedure. Streamlining manufacturing processes for various continuum robots would improve scalability and the feasibility of such systems. Third, integrating autonomous movement with mapping of a patients' individual physiology could yield tremendous benefits in reducing surgical time, fluoroscopy time, and perhaps also minimize tissue damage. The development of autonomous navigation models may prove to be a valuable emergent field. Finally, at the most fundamental level, the miniaturization of motors and overall tool designs, while still providing sufficient force output remains an ever-evolving conundrum.

While these recent innovations point to new challenges – and some consistent ones – they also bring with them new knowledge that will inform the ever-expanding number of approaches. New combinations in hybrid actuation, improved modeling and autonomy, and better device feedback can help propel continuum robots to the front of MIS. A consolidated view of the recent advancements in this field showcases the pertinent trends, and suggests that innovations in robotic surgical systems may help move medical interventions into a new era of data-driven continuum robotics.

# **ACKNOWLEDGMENT**

(Fahad Iqbal and Mojtaba Esfandiari contributed equally to this work.)

# **REFERENCES**

- [1] B. Sawik, S. Tobis, E. Baum, A. Suwalska, S. Kropińska, K. Stachnik, E. Pérez-Bernabeu, M. Cildoz, A. Agustin, and K. Wieczorowska-Tobis, "Robots for elderly care: Review, multi-criteria optimization model and qualitative case study," *Healthcare*, vol. 11, no. 9, p. 1286, Apr. 2023.
- [2] Y. Shen, D. Guo, F. Long, L. A. Mateos, H. Ding, Z. Xiu, R. B. Hellman, A. King, S. Chen, C. Zhang, and H. Tan, "Robots under COVID-19 pandemic: A comprehensive survey," *IEEE Access*, vol. 9, pp. 1590–1615, 2021.
- [3] P. E. Dupont, B. J. Nelson, M. Goldfarb, B. Hannaford, A. Menciassi, M. K. O'Malley, N. Simaan, P. Valdastri, and G.-Z. Yang, "A decade retrospective of medical robotics research from 2010 to 2020," *Sci. Robot.*, vol. 6, no. 60, Nov. 2021, Art. no. eabi8017.
- [4] S. Vadera, A. Chan, T. Lo, A. Gill, A. Morenkova, N. M. Phielipp, N. Hermanowicz, and F. P. K. Hsu, "Frameless stereotactic robot-assisted subthalamic nucleus deep brain stimulation: Case report," World Neurosurg., vol. 97, p. 762, Jan. 2017.

- [5] D. Serletis, J. Bulacio, W. Bingaman, I. Najm, and J. González-Martínez, "The stereotactic approach for mapping epileptic networks: A prospective study of 200 patients," *J. Neurosurg.*, vol. 121, no. 5, pp. 1239–1246, Nov. 2014.
- [6] T. R. K. Varma, P. R. Eldridge, A. Forster, S. Fox, N. Fletcher, M. Steiger, P. Littlechild, P. Byrne, A. Sinnott, K. Tyler, and S. Flintham, "Use of the NeuroMate stereotactic robot in a frameless mode for movement disorder surgery," *Stereotactic Funct. Neurosurg.*, vol. 80, nos. 1–4, pp. 132–135, 2003
- [7] J. Ngu, C. Tsang, and D. Koh, "The da Vinci Xi: A review of its capabilities, versatility, and potential role in robotic colorectal surgery," *Robotic Surg.*, Res. Rev., vol. 4, pp. 77–85, Jul. 2017.
- [8] W. E. Kelley Jr., "The evolution of laparoscopy and the revolution in surgery in the decade of the 1990s," *JSLS*, J. Soc. Laparoendoscopic Surgeons, vol. 12, no. 4, p. 351 2008.
- [9] A. White, M. Skelton, F. Mushtaq, T. Pike, M. Mon-Williams, J. Lodge, and R. Wilkie, "Inconsistent reporting of minimally invasive surgery errors," *Ann. Roy. College Surgeons England*, vol. 97, no. 8, pp. 608–612, Nov. 2015.
- [10] A. D. White, O. Giles, R. J. Sutherland, O. Ziff, M. Mon-Williams, R. M. Wilkie, and J. P. A. Lodge, "Minimally invasive surgery training using multiple port sites to improve performance," *Surgical Endoscopy*, vol. 28, no. 4, pp. 1188–1193, Apr. 2014.
- [11] S. Sadeghnejad, M. Esfandiari, and F. Khadivar, "Chapter 8—A virtual-based haptic endoscopic sinus surgery (ESS) training system: From development to validation," in *Medical and Healthcare Robotics*, O. Boubaker, Ed., Amsterdam, The Netherlands: Elsevier, 2023, pp. 19–201.
- [12] S. Maeso, M. Reza, J. A. Mayol, J. A. Blasco, M. Guerra, E. Andradas, and M. N. Plana, "Efficacy of the da Vinci surgical system in abdominal surgery compared with that of laparoscopy: A systematic review and meta-analysis," *Ann. Surg.*, vol. 252, no. 2, pp. 254–262, Aug. 2010.
- [13] I. D. Walker, "Continuous backbone 'continuum' robot manipulators," Int. Scholarly Res. Notices, vol. 2013, no. 1, 2013, Art. no. 726506.
- [14] J. Burgner-Kahrs, D. C. Rucker, and H. Choset, "Continuum robots for medical applications: A survey," *IEEE Trans. Robot.*, vol. 31, no. 6, pp. 1261–1280, Dec. 2015.
- [15] O. M. Omisore, S. Han, J. Xiong, H. Li, Z. Li, and L. Wang, "A review on flexible robotic systems for minimally invasive surgery," *IEEE Trans. Syst., Man, Cybern., Syst.*, vol. 52, no. 1, pp. 631–644, Jan. 2022.
- [16] P. E. Dupont, N. Simaan, H. Choset, and C. Rucker, "Continuum robots for medical interventions," *Proc. IEEE*, vol. 110, no. 7, pp. 847–870, Jul. 2022.
- [17] Y. Cao, Y. Shi, W. Hong, P. Dai, X. Sun, H. Yu, and L. Xie, "Continuum robots for endoscopic sinus surgery: Recent advances, challenges, and prospects," *Int. J. Med. Robot. Comput. Assist. Surg.*, vol. 19, no. 2, p. e2471, Apr. 2023.
- [18] F. Qi, F. Ju, D. Bai, Y. Wang, and B. Chen, "Motion modelling and error compensation of a cable-driven continuum robot for applications to minimally invasive surgery," *Int. J. Med. Robot. Comput. Assist. Surg.*, vol. 14, no. 6, p. 1932, Dec. 2018.
- [19] M. Brancadoro, M. Manti, F. Grani, S. Tognarelli, A. Menciassi, and M. Cianchetti, "Toward a variable stiffness surgical manipulator based on fiber jamming transition," *Frontiers Robot. AI*, vol. 6, p. 12, Mar. 2019.
- [20] M. Runciman, A. Darzi, and G. P. Mylonas, "Soft robotics in minimally invasive surgery," Soft Robot., vol. 6, no. 4, pp. 423–443, Aug. 2019.
- [21] M. Russo, S. M. H. Sadati, X. Dong, A. Mohammad, I. D. Walker, C. Bergeles, K. Xu, and D. A. Axinte, "Continuum robots: An overview," *Adv. Intell. Syst.*, vol. 5, no. 5, May 2023, Art. no. 2200367.
- [22] I. A. Seleem, H. El-Hussieny, and H. Ishii, "Recent developments of actuation mechanisms for continuum robots: A review," *Int. J. Control, Autom. Syst.*, vol. 21, no. 5, pp. 1592–1609, May 2023.
- [23] Z. Wang, G. Liu, S. Qian, D. Wang, X. Wei, and X. Yu, "Tracking control with external force self-sensing ability based on position/force estimators and non-linear hysteresis compensation for a backdrivable cable-pulleydriven surgical robotic manipulator," *Mechanism Mach. Theory*, vol. 183, May 2023, Art. no. 105259.
- [24] T. Kato, I. Okumura, H. Kose, K. Takagi, and N. Hata, "Tendon-driven continuum robot for neuroendoscopy: Validation of extended kinematic mapping for hysteresis operation," *Int. J. Comput. Assist. Radiol. Surg.*, vol. 11, no. 4, pp. 589–602, Apr. 2016.



- [25] G. Subramani and M. R. Zinn, "Tackling friction—An analytical modeling approach to understanding friction in single tendon driven continuum manipulators," in *Proc. IEEE Int. Conf. Robot. Autom. (ICRA)*, May 2015, pp. 610–617.
- [26] A. Shiva, A. Stilli, Y. Noh, A. Faragasso, I. D. Falco, G. Gerboni, M. Cianchetti, A. Menciassi, K. Althoefer, and H. A. Wurdemann, "Tendon-based stiffening for a pneumatically actuated soft manipulator," *IEEE Robot. Autom. Lett.*, vol. 1, no. 2, pp. 632–637, Jul. 2016.
- [27] J. Shang, D. P. Noonan, C. Payne, J. Clark, M. H. Sodergren, A. Darzi, and G. Z. Yang, "An articulated universal joint based flexible access robot for minimally invasive surgery," in *Proc. IEEE Int. Conf. Robot. Automat.*, May 2011, pp. 1147–1152.
- [28] F. Qi, F. Ju, D. M. Bai, and B. Chen, "Kinematics optimization and static analysis of a modular continuum robot used for minimally invasive surgery," *Proc. Inst. Mech. Eng., H, J. Eng. Med.*, vol. 232, no. 2, pp. 135–148, Feb. 2018.
- [29] B. Ouyang, Y. Liu, and D. Sun, "Design of a three-segment continuum robot for minimally invasive surgery," *Robot. Biomimetics*, vol. 3, no. 1, pp. 1–4, Dec. 2016.
- [30] Z. Wang, S. Bao, B. Zi, Z. Jia, and X. Yu, "Development of a novel 4-DOF flexible endoscopic robot using cable-driven multisegment continuum mechanisms," J. Mech. Robot., vol. 16, no. 3, Mar. 2024, Art. no. 031011.
- [31] E. Amanov, T.-D. Nguyen, and J. Burgner-Kahrs, "Tendon-driven continuum robots with extensible sections—A model-based evaluation of path-following motions," *Int. J. Robot. Res.*, vol. 40, no. 1, pp. 7–23, Jan. 2021.
- [32] T.-D. Nguyen and J. Burgner-Kahrs, "A tendon-driven continuum robot with extensible sections," in *Proc. IEEE/RSJ Int. Conf. Intell. Robots Syst.* (IROS), Sep. 2015, pp. 2130–2135.
- [33] H.-S. Yoon, H.-J. Cha, J. Chung, and B.-J. Yi, "Compact design of a dual master-slave system for maxillary sinus surgery," in *Proc. IEEE/RSJ Int.* Conf. Intell. Robots Syst., Nov. 2013, pp. 5027–5032.
- [34] H.-S. Yoon, J. H. Jeong, and B.-J. Yi, "Image-guided dual master-slave robotic system for maxillary sinus surgery," *IEEE Trans. Robot.*, vol. 34, no. 4, pp. 1098–1111, Aug. 2018.
- [35] J. Wang, C. Hu, G. Ning, L. Ma, X. Zhang, and H. Liao, "A novel miniature spring-based continuum manipulator for minimally invasive surgery: Design and evaluation," *IEEE/ASME Trans. Mechatronics*, vol. 28, no. 5, pp. 2716–2727, Oct. 2023.
- [36] N. Zhang, Y. Kong, H. Huang, S. Song, and B. Li, "Design and kine-matic modeling of a concentric torsionally-steerable flexible surgical robot," in *Proc. IEEE Int. Conf. Robot. Biomimetics (ROBIO)*, Dec. 2022, pp. 2033–2038.
- [37] E. Amanov, T.-D. Nguyen, S. Markmann, F. Imkamp, and J. Burgner-Kahrs, "Toward a flexible variable stiffness endoport for single-site partial nephrectomy," *Ann. Biomed. Eng.*, vol. 46, no. 10, pp. 1498–1510, Oct. 2018.
- [38] M. Hwang and D. Kwon, "K-FLEX: A flexible robotic platform for scar-free endoscopic surgery," *Int. J. Med. Robot. Comput. Assist. Surg.*, vol. 16, no. 2, p. e2078, Apr. 2020.
- [39] M. Hwang and D.-S. Kwon, "Strong continuum manipulator for flexible endoscopic surgery," *IEEE/ASME Trans. Mechatronics*, vol. 24, no. 5, pp. 2193–2203, Oct. 2019.
- [40] W. Hong, L. Xie, J. Liu, Y. Sun, K. Li, and H. Wang, "Development of a novel continuum robotic system for maxillary sinus surgery," *IEEE/ASME Trans. Mechatronics*, vol. 23, no. 3, pp. 1226–1237, Jun. 2018.
- [41] W. Hong, F. Feng, L. Xie, and G.-Z. Yang, "A two-segment continuum robot with piecewise stiffness for maxillary sinus surgery and its decoupling method," *IEEE/ASME Trans. Mechatronics*, vol. 27, no. 6, pp. 4440–4450, Dec. 2022.
- [42] C. F. Graetzel, A. Sheehy, and D. P. Noonan, "Robotic bronchoscopy drive mode of the auris monarch platform," in *Proc. Int. Conf. Robot. Autom. (ICRA)*, May 2019, pp. 3895–3901.
- [43] J. W. Y. Chan, A. T. C. Chang, P. S. Y. Yu, R. W. H. Lau, and C. S. H. Ng, "Robotic assisted-bronchoscopy with cone-beam CT ICG dye marking for lung nodule localization: Experience beyond USA," *Frontiers Surg.*, vol. 9, Jun. 2022, Art. no. 943531.
- [44] S. K. Iwamoto and W. S. Tsai, "Novel approaches utilizing robotic navigational bronchoscopy: A single institution experience," *J. Robotic* Surg., vol. 17, no. 3, pp. 1001–1006, Nov. 2022.

- [45] Z. Yang, X. Zhu, and K. Xu, "Continuum delta robot: A novel translational parallel robot with continuum joints," in *Proc. IEEE/ASME Int. Conf. Adv. Intell. Mechatronics (AIM)*, Jul. 2018, pp. 748–755.
- [46] P. L. Anderson, A. W. Mahoney, and R. J. Webster, "Continuum reconfigurable parallel robots for surgery: Shape sensing and state estimation with uncertainty," *IEEE Robot. Autom. Lett.*, vol. 2, no. 3, pp. 1617–1624, Jul. 2017.
- [47] A. W. Mahoney, P. L. Anderson, P. J. Swaney, F. Maldonado, and R. J. Webster, "Reconfigurable parallel continuum robots for incisionless surgery," in *Proc. IEEE/RSJ Int. Conf. Intell. Robots Syst. (IROS)*, Oct. 2016, pp. 4330–4336.
- [48] A. L. Orekhov, V. A. Aloi, and D. C. Rucker, "Modeling parallel continuum robots with general intermediate constraints," in *Proc. IEEE Int. Conf. Robot. Autom. (ICRA)*, May 2017, pp. 6142–6149.
- [49] C. B. Black, J. Till, and D. C. Rucker, "Parallel continuum robots: Modeling, analysis, and actuation-based force sensing," *IEEE Trans. Robot.*, vol. 34, no. 1, pp. 29–47, Feb. 2018.
- [50] L. Wang and N. Simaan, "Geometric calibration of continuum robots: Joint space and equilibrium shape deviations," *IEEE Trans. Robot.*, vol. 35, no. 2, pp. 387–402, Apr. 2019.
- [51] Y. Xu, D. Song, Z. Zhang, S. Wang, and C. Shi, "A novel extensible continuum robot with growing motion capability inspired by plant growth for path-following in transoral laryngeal surgery," *Soft Robot.*, vol. 11, no. 1, pp. 171–182, Feb. 2024.
- [52] R. J. Webster and B. A. Jones, "Design and kinematic modeling of constant curvature continuum robots: A review," *Int. J. Robot. Res.*, vol. 29, no. 13, pp. 1661–1683, Nov. 2010.
- [53] X. Yang, S. Song, L. Liu, T. Yan, and M. Q. H. Meng, "Design and optimization of concentric tube robots based on surgical tasks, anatomical constraints and follow-the-leader deployment," *IEEE Access*, vol. 7, pp. 173612–173625, 2019.
- [54] D. C. Rucker, R. J. Webster III, G. S. Chirikjian, and N. J. Cowan, "Equilibrium conformations of concentric-tube continuum robots," *Int. J. Robot. Res.*, vol. 29, no. 10, pp. 1263–1280, 2010.
- [55] G. Wu and G. Shi, "Design, modeling, and workspace analysis of an extensible rod-driven parallel continuum robot," *Mechanism Mach. The*ory, vol. 172, Jun. 2022, Art. no. 104798.
- [56] D. T. Friedrich, V. Modes, T. K. Hoffmann, J. Greve, P. J. Schuler, and J. Burgner-Kahrs, "Teleoperated tubular continuum robots for transoral surgery—Feasibility in a porcine larynx model," *Int. J. Med. Robot.* Comput. Assist. Surg., vol. 14, no. 5, p. e1928, Oct. 2018.
- [57] J. Wang, X. Yang, P. Li, S. Song, L. Liu, and M. Q.-H. Meng, "Design of a multi-arm concentric-tube robot system for transnasal surgery," *Med. Biol. Eng. Comput.*, vol. 58, no. 3, pp. 497–508, Mar. 2020.
- [58] T. L. Bruns, A. A. Remirez, M. A. Emerson, R. A. Lathrop, A. W. Mahoney, H. B. Gilbert, C. L. Liu, P. T. Russell, R. F. Labadie, K. D. Weaver, and R. J. Webster, "A modular, multi-arm concentric tube robot system with application to transnasal surgery for orbital tumors," *Int. J. Robot. Res.*, vol. 40, nos. 2–3, pp. 521–533, Feb. 2021.
- [59] H. B. Gilbert, J. Neimat, and R. J. Webster, "Concentric tube robots as steerable needles: Achieving follow-the-leader deployment," *IEEE Trans. Robot.*, vol. 31, no. 2, pp. 246–258, Apr. 2015.
- [60] H. B. Gilbert and R. J. Webster, "Can concentric tube robots follow the leader?" in *Proc. IEEE Int. Conf. Robot. Autom.*, May 2013, pp. 4881–4887.
- [61] H. Su, G. Li, D. C. Rucker, R. J. Webster III, and G. S. Fischer, "A concentric tube continuum robot with piezoelectric actuation for MRI-guided closed-loop targeting," *Ann. Biomed. Eng.*, vol. 44, no. 10, pp. 2863–2873, Oct. 2016.
- [62] H. Su, D. C. Cardona, W. Shang, A. Camilo, G. A. Cole, D. C. Rucker, R. J. Webster, and G. S. Fischer, "A MRI-guided concentric tube continuum robot with piezoelectric actuation: A feasibility study," in *Proc. IEEE Int. Conf. Robot. Autom.*, May 2012, pp. 1939–1945.
- [63] Q. Peyron, Q. Boehler, P. Rougeot, P. Roux, B. J. Nelson, N. Andreff, K. Rabenorosoa, and P. Renaud, "Magnetic concentric tube robots: Introduction and analysis," *Int. J. Robot. Res.*, vol. 41, no. 4, pp. 418–440, Apr. 2022.
- [64] J. Ha and P. E. Dupont, "Designing stable concentric tube robots using piecewise straight tubes," *IEEE Robot. Autom. Lett.*, vol. 2, no. 1, pp. 298–304, Jan. 2017.



- [65] K. A. Xin Jue Luo, T. Looi, S. Sabetian, and J. Drake, "Designing concentric tube manipulators for stability using topology optimization," in *Proc. IEEE/RSJ Int. Conf. Intell. Robots Syst. (IROS)*, Oct. 2018, pp. 1764–1769.
- [66] K. E. Riojas, R. J. Hendrick, and R. J. Webster, "Can elastic instability be beneficial in concentric tube robots?" *IEEE Robot. Autom. Lett.*, vol. 3, no. 3, pp. 1624–1630, Jul. 2018.
- [67] K. Oliver-Butler, J. A. Childs, A. Daniel, and D. C. Rucker, "Concentric push–pull robots: Planar modeling and design," *IEEE Trans. Robot.*, vol. 38, no. 2, pp. 1186–1200, Apr. 2022.
- [68] K. Oliver-Butler, Z. H. Epps, and D. C. Rucker, "Concentric agonistantagonist robots for minimally invasive surgeries," *Proc. SPIE*, vol. 10135, pp. 270–278, Mar. 2017.
- [69] S. Neppalli, B. Jones, W. McMahan, V. Chitrakaran, I. Walker, M. Pritts, M. Csencsits, C. Rahn, and M. Grissom, "OctArm—A soft robotic manipulator," in *Proc. IEEE/RSJ Int. Conf. Intell. Robots Syst.*, Oct. 2007, p. 2569.
- [70] B. Holbrook, M. Csencsits, W. McMahan, V. Chitrakaran, M. Grissom, M. Pritts, B. Jones, C. Rahn, and I. Walker, "Field experiments with the OctArm continuum manipulator," in *Proc. IEEE/RSJ Int. Conf. Intell. Robots Syst.*, Oct. 2006, p. 10.
- [71] S. Maeda, N. Tsujiuchi, T. Koizumi, M. Sugiura, and H. Kojima, "Development and control of a pneumatic robot arm for industrial fields," *Int. J. Adv. Robotic Syst.*, vol. 9, no. 3, p. 59, Sep. 2012.
- [72] A. Arezzo, Y. Mintz, M. E. Allaix, S. Arolfo, M. Bonino, G. Gerboni, M. Brancadoro, M. Cianchetti, A. Menciassi, H. Wurdemann, Y. Noh, K. Althoefer, J. Fras, J. Glowka, Z. Nawrat, G. Cassidy, R. Walker, and M. Morino, "Total mesorectal excision using a soft and flexible robotic arm: A feasibility study in cadaver models," *Surgical Endoscopy*, vol. 31, no. 1, pp. 264–273, Jan. 2017.
- [73] M. Cianchetti, T. Ranzani, G. Gerboni, I. De Falco, C. Laschi, and A. Menciassi, "STIFF-FLOP surgical manipulator: Mechanical design and experimental characterization of the single module," in *Proc.* IEEE/RSJ Int. Conf. Intell. Robots Syst., Nov. 2013, pp. 3576–3581.
- [74] M. Cianchetti, T. Ranzani, G. Gerboni, T. Nanayakkara, K. Althoefer, P. Dasgupta, and A. Menciassi, "Soft robotics technologies to address shortcomings in today's minimally invasive surgery: The STIFF-FLOP approach," Soft Robot., vol. 1, no. 2, pp. 122–131, Jun. 2014.
- [75] N. Pagliarani, L. Arleo, S. Albini, and M. Cianchetti, "Variable stiffness technologies for soft robotics: A comparative approach for the STIFF-FLOP manipulator," *Actuators*, vol. 12, no. 3, p. 96, Feb. 2023.
- [76] F. Renda, M. Cianchetti, H. Abidi, J. Dias, and L. Seneviratne, "Screw-based modeling of soft manipulators with tendon and fluidic actuation," J. Mech. Robot., vol. 9, no. 4, Aug. 2017, Art. no. 041012.
- [77] X. Chen, J. Shi, H. Wurdemann, and T. G. Thuruthel, "Vision-based tip force estimation on a soft continuum robot," in *Proc. IEEE Int. Conf. Robot. Autom. (ICRA)*, May 2024, pp. 7621–7627.
- [78] P. Chaillou, J. Shi, A. Kruszewski, I. Fournier, H. A. Wurdemann, and C. Duriez, "Reduced finite element modelling and closed-loop control of pneumatic-driven soft continuum robots," in *Proc. IEEE Int. Conf. Soft Robot. (RoboSoft)*, Apr. 2023, pp. 1–8.
- [79] N. Garbin, L. Wang, J. H. Chandler, K. L. Obstein, N. Simaan, and P. Valdastri, "A disposable continuum endoscope using piston-driven parallel bellow actuator," in *Proc. Int. Symp. Med. Robot. (ISMR)*, Mar. 2018, pp. 1–6.
- [80] N. Garbin, L. Wang, J. H. Chandler, K. L. Obstein, N. Simaan, and P. Valdastri, "Dual-continuum design approach for intuitive and low-cost upper gastrointestinal endoscopy," *IEEE Trans. Biomed. Eng.*, vol. 66, no. 7, pp. 1963–1974, Jul. 2019.
- [81] B. Gorissen, M. De Volder, and D. Reynaerts, "Chip-on-tip endoscope incorporating a soft robotic pneumatic bending microactuator," *Biomed. Microdevices*, vol. 20, no. 3, p. 73, Sep. 2018.
- [82] G. Chen, M. Tu Pham, and T. Redarce, "A semi-autonomous microrobotic system for colonoscopy," in *Proc. IEEE Int. Conf. Robot. Biomimetics*, Feb. 2009, pp. 703–708.
- [83] G. Chen, L. Fu, M. T. Pham, and T. Redarce, "Characterization and modeling of a pneumatic actuator for a soft continuum robot," in *Proc. IEEE Int. Conf. Mechatronics Autom.*, Aug. 2013, pp. 243–248.
- [84] M. De Volder and D. Reynaerts, "Pneumatic and hydraulic microactuators: A review," J. Micromech. Microeng., vol. 20, no. 4, Apr. 2010, Art. no. 043001.

- [85] D. Haraguchi, T. Kanno, K. Tadano, and K. Kawashima, "A pneumatically driven surgical manipulator with a flexible distal joint capable of force sensing," *IEEE/ASME Trans. Mechatronics*, vol. 20, no. 6, pp. 2950–2961, Dec. 2015.
- [86] L. Lindenroth, C. Duriez, J. Back, K. Rhode, and H. Liu, "Intrinsic force sensing capabilities in compliant robots comprising hydraulic actuation," in *Proc. IEEE/RSJ Int. Conf. Intell. Robots Syst. (IROS)*, Sep. 2017, pp. 2923–2928.
- [87] L. Lindenroth, J. Back, A. Schoisengeier, Y. Noh, H. Würdemann, K. Althoefer, and H. Liu, "Stiffness-based modelling of a hydraulicallyactuated soft robotics manipulator," in *Proc. IEEE/RSJ Int. Conf. Intell. Robots Syst. (IROS)*, Oct. 2016, pp. 2458–2463.
- [88] R. Stopforth, S. Davrajh, and K. Althoefer, "Low cost soft endoscope robotic probe," in *Proc. IEEE AFRICON*, Sep. 2017, pp. 1414–1419.
- [89] F. Campisano, A. A. Remirez, C. A. Landewee, S. Caló, K. L. Obstein, R. J. Webster, and P. Valdastri, "Teleoperation and contact detection of a waterjet-actuated soft continuum manipulator for low-cost gastroscopy," *IEEE Robot. Autom. Lett.*, vol. 5, no. 4, pp. 6427–6434, Oct. 2020.
- [90] M. Vasina, F. Solc, and K. Hoder, "Shape memory alloys—unconventional actuators," in *Proc. IEEE Int. Conf. Ind. Technol.*, Dec. 2003, pp. 190–193.
- [91] D.-S. Copaci, D. Blanco, A. Martin-Clemente, and L. Moreno, "Flexible shape memory alloy actuators for soft robotics: Modelling and control," *Int. J. Adv. Robotic Syst.*, vol. 17, no. 1, Jan. 2020, Art. no. 1729881419886747.
- [92] J. O. Alcaide, L. Pearson, and M. E. Rentschler, "Design, modeling and control of a SMA-actuated biomimetic robot with novel functional skin," in *Proc. IEEE Int. Conf. Robot. Autom. (ICRA)*, May 2017, pp. 4338–4345.
- [93] J. Sheng, D. Gandhi, R. Gullapalli, J. M. Simard, and J. P. Desai, "Development of a meso-scale SMA-based torsion actuator for image-guided procedures," *IEEE Trans. Robot.*, vol. 33, no. 1, pp. 240–248, Feb. 2017.
- [94] J. Sheng and J. P. Desai, "Towards a SMA-actuated neurosurgical intracerebral hemorrhage evacuation (NICHE) robot," in *Proc. IEEE/RSJ Int. Conf. Intell. Robots Syst. (IROS)*, Sep. 2015, pp. 3805–3810.
- [95] J. Sheng and J. P. Desai, "A novel meso-scale SMA-actuated torsion actuator," in *Proc. IEEE/RSJ Int. Conf. Intell. Robots Syst. (IROS)*, Oct. 2015, pp. 4718–4723.
- [96] Y. Kim, S. S. Cheng, and J. P. Desai, "Active stiffness tuning of a spring-based continuum robot for MRI-guided neurosurgery," *IEEE Trans. Robot.*, vol. 34, no. 1, pp. 18–28, Feb. 2018.
- [97] M. A. Mandolino, Y. Goergen, P. Motzki, and G. Rizzello, "Design and characterization of a fully integrated continuum robot actuated by shape memory alloy wires," in *Proc. IEEE 17th Int. Conf. Adv. Motion Control* (AMC), Feb. 2022, pp. 6–11.
- [98] Q. Wang, L. Yan, M. Li, H. Li, and B. Zhang, "Reliability analysis of continuum robot actuated by shape memory alloy (SMA)," in *Proc. 6th Int. Conf. Autom., Control Robot. Eng. (CACRE)*, Jul. 2021, pp. 97–101.
- [99] T. A. U. Roshan, Y. W. R. Amarasinghe, and N. W. N. Dayananda, "Design and development of a shape memory alloy spring actuated gripper for minimally invasive surgeries," in *Proc. Int. Conf. Artif. Life Robot.*, vol. 23, Feb. 2018, pp. 566–569.
- [100] U. Roshan, J. B. Basnayake, R. Amarasinghe, and N. Dayananda, "Design and development of a force feedback system for a SMA based gripper as a minimally invasive surgical tool," in *Proc. IEEE SENSORS*, Oct. 2019, pp. 1–4.
- [101] Q. Ding, Y. Lu, A. Kyme, and S. S. Cheng, "Towards a multi-imager compatible continuum robot with improved dynamics driven by modular SMA," in *Proc. IEEE Int. Conf. Robot. Autom. (ICRA)*, May 2021, pp. 11930–11937.
- [102] A. Diodato, M. Brancadoro, G. De Rossi, H. Abidi, D. Dall'Alba, R. Muradore, G. Ciuti, P. Fiorini, A. Menciassi, and M. Cianchetti, "Soft robotic manipulator for improving dexterity in minimally invasive surgery," *Surgical Innov.*, vol. 25, no. 1, pp. 69–76, Feb. 2018.
- [103] P. Lloyd, A. K. Hoshiar, T. da Veiga, A. Attanasio, N. Marahrens, J. H. Chandler, and P. Valdastri, "A learnt approach for the design of magnetically actuated shape forming soft tentacle robots," *IEEE Robot. Autom. Lett.*, vol. 5, no. 3, pp. 3937–3944, Jul. 2020.
- [104] T. L. Thomas, J. Bos, J. J. Huaroto, V. Kalpathy Venkiteswaran, and S. Misra, "A magnetically actuated variable stiffness manipulator based on deployable shape memory polymer springs," *Adv. Intell. Syst.*, vol. 6, no. 2, Feb. 2024, Art. no. 2200465.



- [105] X. Hu, A. Chen, Y. Luo, C. Zhang, and E. Zhang, "Steerable catheters for minimally invasive surgery: A review and future directions," *Comput. Assist. Surg.*, vol. 23, no. 1, pp. 21–41, Jan. 2018.
- [106] G. R. Sutherland, I. Latour, A. D. Greer, T. Fielding, G. Feil, and P. Newhook, "An image-guided magnetic resonance-compatible surgical robot," *Neurosurgery*, vol. 62, no. 2, pp. 286–293, Feb. 2008.
- [107] Z. Koszowska, M. Brockdorff, T. da Veiga, G. Pittiglio, P. Lloyd, T. Khan-White, R. A. Harris, J. W. Moor, J. H. Chandler, and P. Valdastri, "Independently actuated soft magnetic manipulators for bimanual operations in confined anatomical cavities," *Adv. Intell. Syst.*, vol. 6, no. 2, Feb. 2024. Art. no. 2300062.
- [108] S. O. Poore, "The morphological basis of the arm-to-wing transition," J. Hand Surg., vol. 33, no. 2, pp. 277–280, Feb. 2008.
- [109] P. Hunter, "Turning nature's inspiration into a production line," EMBO Rep., vol. 15, no. 11, pp. 1123–1127, Nov. 2014.
- [110] B. Lin, S. Song, and J. Wang, "Variable stiffness methods of flexible robots for minimally invasive surgery: A review," *Biomimetic Intell. Robot.*, vol. 4, no. 3, Sep. 2024, Art. no. 100168.
- [111] L. Blanc, A. Delchambre, and P. Lambert, "Flexible medical devices: Review of controllable stiffness solutions," *Actuators*, vol. 6, no. 3, p. 23, Jul. 2017.
- [112] W. Dou, G. Zhong, J. Cao, Z. Shi, B. Peng, and L. Jiang, "Soft robotic manipulators: Designs, actuation, stiffness tuning, and sensing," Adv. Mater. Technol., vol. 6, no. 9, Sep. 2021, Art. no. 2100018.
- [113] Y. Fan, B. Yi, and D. Liu, "An overview of stiffening approaches for continuum robots," *Robot. Comput.-Integr. Manuf.*, vol. 90, Dec. 2024, Art. no. 102811.
- [114] M. Langer, E. Amanov, and J. Burgner-Kahrs, "Stiffening sheaths for continuum robots," Soft Robot., vol. 5, no. 3, pp. 291–303, Jun. 2018.
- [115] J. S. Mehling, M. A. Diftler, M. Chu, and M. Valvo, "A minimally invasive tendril robot for in-space inspection," in *Proc. 1st IEEE/RAS-EMBS Int. Conf. Biomed. Robot. Biomechatronics*, Feb. 2006, pp. 690–695.
- [116] J. L. C. Santiago, I. D. Walker, and I. S. Godage, "Continuum robots for space applications based on layer-jamming scales with stiffening capability," in *Proc. IEEE Aerosp. Conf.*, Mar. 2015, pp. 1–13.
- [117] S. M. H. Sadati, Y. Noh, S. E. Naghibi, K. Althoefer, and T. Nanayakkara, "Stiffness control of soft robotic manipulator for minimally invasive surgery (MIS) using scale jamming," in *Proc. Intell. Robot. Appl.*, 9th Int. Conf., 2015, pp. 141–151.
- [118] D. C. F. Li, Z. Wang, B. Ouyang, and Y.-H. Liu, "A reconfigurable variable stiffness manipulator by a sliding layer mechanism," in *Proc. Int. Conf. Robot. Autom. (ICRA)*, May 2019, pp. 3976–3982.
- [119] H. Abidi, G. Gerboni, M. Brancadoro, J. Fras, A. Diodato, M. Cianchetti, H. Wurdemann, K. Althoefer, and A. Menciassi, "Highly dexterous 2-module soft robot for intra-organ navigation in minimally invasive surgery," *Int. J. Med. Robot. Comput. Assist. Surg.*, vol. 14, no. 1, p. e1875, Feb. 2018.
- [120] I. Tamadon, Y. Huan, A. G. de Groot, A. Menciassi, and E. Sinibaldi, "Positioning and stiffening of an articulated/continuum manipulator for implant delivery in minimally invasive surgery," *Int. J. Med. Robot. Comput. Assist. Surg.*, vol. 16, no. 2, p. e2072, Apr. 2020.
- [121] J. Kim, W.-Y. Choi, S. Kang, C. Kim, and K.-J. Cho, "Continuously variable stiffness mechanism using nonuniform patterns on coaxial tubes for continuum microsurgical robot," *IEEE Trans. Robot.*, vol. 35, no. 6, pp. 1475–1487, Dec. 2019.
- [122] Q. Jacquemin, Q. Sun, D. Thuau, E. Monteiro, S. Tence-Girault, and N. Mechbal, "Design of a new electroactive polymer based continuum actuator for endoscopic surgical robots," in *Proc. IEEE/RSJ Int. Conf. Intell. Robots Syst. (IROS)*, Oct. 2020, pp. 3208–3215.
- [123] D. Fleck, H. Albadawi, F. Shamoun, G. Knuttinen, S. Naidu, and R. Oklu, "Catheter-directed thrombolysis of deep vein thrombosis: Literature review and practice considerations," *Cardiovascular Diagnosis Therapy*, vol. 7, no. 3, pp. 228–237, Dec. 2017.
- [124] S. I. Ahmed, G. Javed, S. B. Bareeqa, S. S. Samar, A. Shah, A. Giani, Z. Aziz, A. Tasleem, and S. H. Humayun, "Endovascular coiling versus neurosurgical clipping for aneurysmal subarachnoid hemorrhage: A systematic review and meta-analysis," *Cureus*, vol. 11, no. 3, p. e4320, Mar. 2019.
- [125] J. S. Uchiyamada, S. Ichihashi, S. Iwakoshi, H. Itoh, N. Tabayashi, and K. Kichikawa, "Technical tips and procedural steps in endovascular aortic aneurysm repair with concomitant recanalization of iliac artery occlusions," *SpringerPlus*, vol. 2, no. 1, pp. 1–5, Dec. 2013.

- [126] A. R. Tzafriri and E. R. Edelman, "Endovascular drug delivery and drug elution systems: First principles," *Interventional Cardiol. Clinics*, vol. 5, no. 3, p. 307, 2016.
- [127] K. Yamagata, B. Aldhoon, and J. Kautzner, "Reduction of fluoroscopy time and radiation dosage during catheter ablation for atrial fibrillation," *Arrhythmia Electrophysiol. Rev.*, vol. 5, no. 2, p. 144, 2016.
- [128] M. Ragosta and K. P. Singh, "Robotic-assisted percutaneous coronary intervention: Rationale, implementation, case selection and limitations of current technology," *J. Clin. Med.*, vol. 7, no. 2, p. 23, Jan. 2018.
- [129] G. Bassil, C. F. Liu, S. M. Markowitz, G. Thomas, J. E. Ip, C. Macatangay, T. Maglione, L. Saleh, B. B. Lerman, and J. W. Cheung, "Comparison of robotic magnetic navigation-guided and manual catheter ablation of ventricular arrhythmias arising from the papillary muscles," *EP Europace*, vol. 20, pp. 5–10, May 2018.
- [130] W. Ullah, R. J. Hunter, S. Haldar, A. Mclean, M. Dhinoja, S. Sporton, M. J. Earley, F. Lorgat, T. Wong, and R. J. Schilling, "Comparison of robotic and manual persistent AF ablation using catheter contact force sensing: An international multicenter registry study," *Pacing Clin. Elec*trophysiol., vol. 37, no. 11, pp. 1427–1435, Nov. 2014.
- [131] S. K. Huang and J. M. Miller, Catheter Ablation of Cardiac Arrhythmias, 4th ed., Amsterdam, The Netherlands: Elsevier, 2019, p. 703.
- [132] W. Cheng and P. K. Law, "Conceptual design and procedure for an autonomous intramyocardial injection catheter," *Cell Transplantation*, vol. 26, no. 5, pp. 735–751, May 2017.
- [133] W. Cheng and P. K. Law, "Feedforward coordinate control of a robotic cell injection catheter," *Cell Transplantation*, vol. 26, no. 8, pp. 1319–1330, Aug. 2017.
- [134] K. Yoshimitsu, T. Kato, S.-E. Song, and N. Hata, "A novel four-wire-driven robotic catheter for radio-frequency ablation treatment," *Int. J. Comput. Assist. Radiol. Surg.*, vol. 9, no. 5, pp. 867–874, Sep. 2014.
- [135] M. Jolaei, A. Hooshiar, J. Dargahi, and M. Packirisamy, "Toward task autonomy in robotic cardiac ablation: Learning-based kinematic control of soft tendon-driven catheters," *Soft Robot.*, vol. 8, no. 3, pp. 340–351, Jun. 2021.
- [136] G. Fagogenis, M. Mencattelli, Z. Machaidze, B. Rosa, K. Price, F. Wu, V. Weixler, M. Saeed, J. E. Mayer, and P. E. Dupont, "Autonomous robotic intracardiac catheter navigation using haptic vision," *Sci. Robot.*, vol. 4, no. 29, Apr. 2019, Art. no. eaaw1977.
- [137] C. Girerd, A. V. Kudryavtsev, P. Rougeot, P. Renaud, K. Rabenorosoa, and B. Tamadazte, "SLAM-based follow-the-leader deployment of concentric tube robots," *IEEE Robot. Autom. Lett.*, vol. 5, no. 2, pp. 548–555, Apr. 2020.
- [138] Y. Inoue and K. Ikuta, "Hydraulic driven active catheters with optical bending sensor," in *Proc. IEEE 29th Int. Conf. Micro Electro Mech. Syst.* (MEMS), Jan. 2016, pp. 383–386.
- [139] K. Ikuta, Y. Matsuda, D. Yajima, and Y. Ota, "Pressure pulse drive: A control method for the precise bending of hydraulic active catheters," *IEEE/ASME Trans. Mechatronics*, vol. 17, no. 5, pp. 876–883, Oct. 2012.
- [140] Y. Haga, Y. Muyari, T. Mineta, T. Matsunaga, H. Akahori, and M. Esashi, "Small diameter hydraulic active bending catheter using laser processed super elastic alloy and silicone rubber tube," in *Proc. 3rd IEEE/EMBS* Special Topic Conf. Microtechnology Med. Biol., May 2005, pp. 245–248.
- [141] C. C. Nguyen, T. Teh, M. T. Thai, P. T. Phan, T. T. Hoang, J. Davies, H.-P. Phan, C. H. Wang, N. H. Lovell, and T. N. Do, "A handheld hydraulic soft robotic device with bidirectional bending end-effector for minimally invasive surgery," *IEEE Trans. Med. Robot. Bionics*, vol. 5, no. 3, pp. 590–601, Aug. 2023.
- [142] C. C. Nguyen, M. T. Thai, T. T. Hoang, J. Davies, P. T. Phan, K. Zhu, L. Wu, M. A. Brodie, D. Tsai, Q. P. Ha, H.-P. Phan, N. H. Lovell, and T. N. Do, "Development of a soft robotic catheter for vascular intervention surgery," *Sens. Actuators A, Phys.*, vol. 357, Aug. 2023, Art. no. 114380.
- [143] Y.-H. Lu, K. Mani, B. Panigrahi, S. Hajari, and C.-Y. Chen, "A shape memory alloy-based miniaturized actuator for catheter interventions," *Cardiovascular Eng. Technol.*, vol. 9, no. 3, pp. 405–413, Sep. 2018.
- [144] S. Shao, B. Sun, Q. Ding, W. Yan, W. Zheng, K. Yan, Y. Hong, and S. S. Cheng, "Design, modeling, and control of a compact SMA-actuated MR-conditional steerable neurosurgical robot," *IEEE Robot. Autom. Lett.*, vol. 5, no. 2, pp. 1381–1388, Apr. 2020.
- [145] V. Woehling, G. T. M. Nguyen, C. Plesse, M. Farajollahi, J. D. W. Madden, and F. Vidal, "Toward electroactive catheter design using conducting interpenetrating polymer networks actuators," *Proc.* SPIE, vol. 10594, pp. 222–228, mar. 2018.



- [146] F. Ganet, M. Q. Le, J. F. Capsal, P. Lermusiaux, L. Petit, A. Millon, and P. J. Cottinet, "Development of a smart guide wire using an electrostrictive polymer: Option for steerable orientation and force feedback," *Sci. Rep.*, vol. 5, no. 1, p. 18593, Dec. 2015.
- [147] Q. Jacquemin, Q. Sun, D. Thuau, E. Monteiro, S. Tence-Girault, S. Doizi, O. Traxer, and N. Mechbal, "Design and control of a new electrostrictive polymer based continuum actuator for endoscopic robot," *J. Intell. Mater. Syst. Struct.*, vol. 34, no. 12, pp. 1355–1365, Jul. 2023.
- [148] D. Filgueiras-Rama, A. Estrada, J. Shachar, S. Castrejón, D. Doiny, M. Ortega, E. Gang, and J. L. Merino, "Remote magnetic navigation for accurate, real-time catheter positioning and ablation in cardiac electrophysiology procedures," *J. Visualized Experiments*, no. 74, p. 3658, Apr. 2013.
- [149] F. Kiemeneij, M. S. Patterson, G. Amoroso, G. Laarman, and T. Slagboom, "Use of the stereotaxis Niobe<sup>®</sup> magnetic navigation system for percutaneous coronary intervention: Results from 350 consecutive patients," *Catheterization Cardiovascular Interventions*, vol. 71, no. 4, pp. 510–516, Mar. 2008.
- [150] A. Da Costa, J. B. Guichard, N. Maillard, C. Romeyer-Bouchard, A. Gerbay, and K. Isaaz, "Substantial superiority of Niobe ES over Niobe II system in remote-controlled magnetic pulmonary vein isolation," *Int. J. Cardiol.*, vol. 230, pp. 319–323, Mar. 2017.
- [151] (2020). Stereotaxis. [Online]. Available: http://www.stereotaxis.com/ products/
- [152] Y. Kim, G. A. Parada, S. Liu, and X. Zhao, "Ferromagnetic soft continuum robots," Sci. Robot., vol. 4, no. 33, Aug. 2019, Art. no. eaax7329.
- [153] C. Chautems, A. Tonazzini, D. Floreano, and B. J. Nelson, "A variable stiffness catheter controlled with an external magnetic field," in *Proc. IEEE/RSJ Int. Conf. Intell. Robots Syst. (IROS)*, Sep. 2017, pp. 181–186.
- [154] C. Chautems, A. Tonazzini, Q. Boehler, S. H. Jeong, D. Floreano, and B. J. Nelson, "Magnetic continuum device with variable stiffness for minimally invasive surgery," *Adv. Intell. Syst.*, vol. 2, no. 6, Jun. 2020, Art. no. 1900086.
- [155] N. Kim, S. Lee, W. Lee, and G. Jang, "Development of a magnetic catheter with rotating multi-magnets to achieve unclogging motions with enhanced steering capability," AIP Adv., vol. 8, no. 5, May 2018, Art. no. 056708.
- [156] T. Liu, N. Lombard Poirot, T. Greigarn, and M. Cenk Çavuşoğlu, "Design of a magnetic resonance imaging guided magnetically actuated steerable catheter," J. Med. Devices, vol. 11, no. 2, Jun. 2017, Art. no. 0210041.
- [157] M. Ilami, R. J. Ahmed, A. Petras, B. Beigzadeh, and H. Marvi, "Magnetic needle steering in soft phantom tissue," *Sci. Rep.*, vol. 10, no. 1, p. 2500, Feb. 2020.
- [158] E. Jung, W. Lee, N. Kim, J. Kim, J. Park, and G. Jang, "Enhanced steering ability of the distal end of a magnetic catheter by utilizing magnets with optimized magnetization direction," AIP Adv., vol. 9, no. 12, Dec. 2019, Art. no. 125230.
- [159] P. Ryan and E. Diller, "Five-degree-of-freedom magnetic control of micro-robots using rotating permanent magnets," in *Proc. IEEE Int. Conf. Robot. Autom. (ICRA)*, May 2016, pp. 1731–1736.
- [160] Y. Piskarev, Y. Sun, M. Righi, Q. Boehler, C. Chautems, C. Fischer, B. J. Nelson, J. Shintake, and D. Floreano, "Fast-response variablestiffness magnetic catheters for minimally invasive surgery," Adv. Sci., vol. 11, no. 12, Mar. 2024, Art. no. 2305537.
- [161] M. Mattmann, Q. Boehler, X.-Z. Chen, S. Pané, and B. J. Nelson, "Shape memory polymer variable stiffness magnetic catheters with hybrid stiffness control," in *Proc. IEEE/RSJ Int. Conf. Intell. Robots Syst. (IROS)*, Oct. 2022, pp. 9589–9595.
- [162] L. Mao, P. Yang, C. Tian, X. Shen, F. Wang, H. Zhang, X. Meng, and H. Xie, "Magnetic steering continuum robot for transluminal procedures with programmable shape and functionalities," *Nature Commun.*, vol. 15, no. 1, p. 3759, May 2024.
- [163] F. A. Jolesz, "Intraoperative imaging in neurosurgery: Where will the future take us?" Acta Neurochir Suppl., vol. 109, pp. 21–25, Jan. 2011.
- [164] B. Axelsson, "Optimisation in fluoroscopy," *Biomed. Imag. Intervent J.*, vol. 3, no. 2, p. e47, Apr. 2007.
- [165] M. Goyal, G. R. Sutherland, S. Lama, P. Cimflova, N. Kashani, A. Mayank, M.-N. Psychogios, L. Spelle, V. Costalat, N. Sakai, and J. M. Ospel, "Neurointerventional robotics: Challenges and opportunities," *Clin. Neuroradiol.*, vol. 30, no. 2, pp. 203–208, Jun. 2020.

- [166] C. Shi, X. Luo, P. Qi, T. Li, S. Song, Z. Najdovski, T. Fukuda, and H. Ren, "Shape sensing techniques for continuum robots in minimally invasive surgery: A survey," *IEEE Trans. Biomed. Eng.*, vol. 64, no. 8, pp. 1665–1678, Aug. 2017.
- [167] A. Ramadani, M. Bui, T. Wendler, H. Schunkert, P. Ewert, and N. Navab, "A survey of catheter tracking concepts and methodologies," *Med. Image Anal.*, vol. 82, Nov. 2022, Art. no. 102584.
- [168] D. L. Miller, "Overview of contemporary interventional fluoroscopy procedures," *Health Phys.*, vol. 95, no. 5, pp. 638–644, Nov. 2008.
- [169] J. J. Pasternak and E. E. Williamson, "Clinical pharmacology, uses, and adverse reactions of iodinated contrast agents: A primer for the nonradiologist," *Mayo Clinic Proc.*, vol. 87, no. 4, pp. 390–402, Apr. 2012.
- [170] M. Mahesh, "Fluoroscopy: Patient radiation exposure issues," *Radio-Graphics*, vol. 21, no. 4, pp. 1033–1045, Jul. 2001.
- [171] E. J. Lobaton, J. Fu, L. G. Torres, and R. Alterovitz, "Continuous shape estimation of continuum robots using X-ray images," in *Proc. IEEE Int. Conf. Robot. Automat.*, May 2013, pp. 725–732.
- [172] T. A. Brumfiel, R. Qi, S. Ravigopal, and J. P. Desai, "Image-based force localization and estimation of a micro-scale continuum guidewire robot," *IEEE Trans. Med. Robot. Bionics*, vol. 6, no. 1, pp. 153–162, Feb. 2024.
- [173] L. Rui, "Model-based lasso catheter tracking in monoplane fluoroscopy for 3D breathing motion compensation during EP procedures," *Proc.* SPIE, vol. 7625, pp. 297–303, Feb. 2010.
- [174] M. Wagner, S. Schafer, C. Strother, and C. Mistretta, "4D interventional device reconstruction from biplane fluoroscopy," *Med. Phys.*, vol. 43, no. 3, pp. 1324–1334, Mar. 2016.
- [175] C. S. Hong, Z. C. Chen, K. T. Tang, and W. T. Chang, "The effectiveness and safety between monoplane and biplane imaging during coronary angiographies," *Acta Cardiologica Sinica*, vol. 36, no. 2, p. 105, 2020.
- [176] D.-K. Jang, D. A. Stidd, S. Schafer, M. Chen, R. Moftakhar, and D. K. Lopes, "Monoplane 3D overlay roadmap versus conventional biplane 2D roadmap technique for neurointervenional procedures," *Neurointervention*, vol. 11, no. 2, pp. 105–113, 2016.
- [177] Y. Ma, N. Gogin, P. Cathier, R. J. Housden, G. Gijsbers, M. Cooklin, M. O'Neill, J. Gill, C. A. Rinaldi, R. Razavi, and K. S. Rhode, "Real-time X-ray fluoroscopy-based catheter detection and tracking for cardiac electrophysiology interventions," *Med. Phys.*, vol. 40, no. 7, Jul. 2013, Art. no. 071902.
- [178] M. G. Wagner, C. M. Strother, and C. A. Mistretta, "Guidewire path tracking and segmentation in 2D fluoroscopic time series using device paths from previous frames," *Proc. SPIE*, vol. 9784, pp. 621–627, Mar. 2016.
- [179] C. L. Merdes and P. D. Wolf, "Locating a catheter transducer in a three-dimensional ultrasound imaging field," *IEEE Trans. Biomed. Eng.*, vol. 48, no. 12, pp. 1444–1452, Dec. 2001.
- [180] G. J. Vrooijink, M. Abayazid, and S. Misra, "Real-time three-dimensional flexible needle tracking using two-dimensional ultrasound," in *Proc. IEEE Int. Conf. Robot. Autom.*, May 2013, pp. 1688–1693.
- [181] Z. Li, X. Yang, S. Song, L. Liu, and M. Q.-H. Meng, "Tip estimation approach for concentric tube robots using 2D ultrasound images and kinematic model," *Med. Biol. Eng. Comput.*, vol. 59, nos. 7–8, pp. 1461–1473, Aug. 2021.
- [182] R. Razavi, D. L. Hill, S. F. Keevil, M. E. Miquel, V. Muthurangu, S. Hegde, K. Rhode, M. Barnett, J. van Vaals, D. J. Hawkes, and E. Baker, "Cardiac catheterisation guided by MRI in children and adults with congenital heart disease," *Lancet*, vol. 362, no. 9399, pp. 1877–1882, Dec. 2003.
- [183] J. A. Bell, C. E. Saikus, K. Ratnayaka, V. Wu, M. Sonmez, A. Z. Faranesh, J. H. Colyer, R. J. Lederman, and O. Kocaturk, "A deflectable guiding catheter for real-time MRI-guided interventions," *J. Magn. Reson. Imag.*, vol. 35, no. 4, pp. 908–915, Apr. 2012.
- [184] X. Li, L. E. Perotti, J. A. Martinez, S. M. Duarte-Vogel, D. B. Ennis, and H. H. Wu, "Real-time 3T MRI-guided cardiovascular catheterization in a porcine model using a glass-fiber epoxy-based guidewire," *PLoS ONE*, vol. 15, no. 2, Feb. 2020, Art. no. e0229711.
- [185] T. Heidt, S. Reiss, A. J. Krafft, A. Ç. Özen, T. Lottner, C. Hehrlein, R. Galmbacher, G. Kayser, I. Hilgendorf, P. Stachon, D. Wolf, A. Zirlik, K. Düring, M. Zehender, S. Meckel, D. V. Elverfeldt, C. Bode, M. Bock, and C. V. Z. Mühlen, "Real-time magnetic resonance imaging—Guided coronary intervention in a porcine model," *Sci. Rep.*, vol. 9, no. 1, p. 8663, Jun. 2019.



- [186] A. Massmann, A. Buecker, and G. K. Schneider, "Glass-fiber-based MR-safe guidewire for MR imaging-guided endovascular interventions: In vitro and preclinical in vivo feasibility study," *Radiology*, vol. 284, no. 2, pp. 541–551, Aug. 2017.
- [187] A. E. Campbell-Washburn, T. Rogers, A. M. Stine, J. M. Khan, R. Ramasawmy, W. H. Schenke, D. R. McGuirt, J. R. Mazal, L. P. Grant, E. K. Grant, D. A. Herzka, and R. J. Lederman, "Right heart catheterization using metallic guidewires and low SAR cardiovascular magnetic resonance fluoroscopy at 1.5 tesla: First in human experience," *J. Car-diovascular Magn. Reson.*, vol. 20, no. 1, p. 41, Feb. 2018.
- [188] K. E. Schleicher, M. Bock, K. Düring, S. Kroboth, and A. J. Krafft, "Radial MRI with variable echo times: Reducing the orientation dependency of susceptibility artifacts of an MR-safe guidewire," *Magn. Reson. Mater. Phys., Biol. Med.*, vol. 31, no. 2, pp. 235–242, Apr. 2018.
- [189] B. Basar, T. Rogers, K. Ratnayaka, A. E. Campbell-Washburn, J. R. Mazal, W. H. Schenke, M. Sonmez, A. Z. Faranesh, R. J. Lederman, and O. Kocaturk, "Segmented nitinol guidewires with stiffness-matched connectors for cardiovascular magnetic resonance catheterization: Preserved mechanical performance and freedom from heating," *J. Cardio*vascular Magn. Reson., vol. 17, no. 1, p. 105, Jan. 2015.
- [190] K. D. Yildirim, B. Basar, A. E. Campbell-Washburn, D. A. Herzka, O. Kocaturk, and R. J. Lederman, "A cardiovascular magnetic resonance (CMR) safe metal braided catheter design for interventional CMR at 1.5 T: Freedom from radiofrequency induced heating and preserved mechanical performance," *J. Cardiovascular Magn. Reson.*, vol. 21, no. 1, p. 16, Jan. 2019.
- [191] K. Pushparajah, H. Chubb, and R. Razavi, "MR-guided cardiac interventions," *Topics Magn. Reson. Imag.*, vol. 27, no. 3, pp. 115–128, Jun. 2018.
- [192] R. K. Mukherjee, H. Chubb, S. Roujol, R. Razavi, and M. D. O'Neill, "Advances in real-time MRI-guided electrophysiology," *Current Cardiovascular Imag. Rep.*, vol. 12, no. 2, pp. 1–10, Feb. 2019.
- [193] A. E. Campbell-Washburn, M. A. Tavallaei, M. Pop, E. K. Grant, H. Chubb, K. Rhode, and G. A. Wright, "Real-time MRI guidance of cardiac interventions," *J. Magn. Reson. Imag.*, vol. 46, no. 4, pp. 935–950, Oct. 2017.
- [194] L. Dupourqué, F. Masaki, Y. L. Colson, T. Kato, and N. Hata, "Transbronchial biopsy catheter enhanced by a multisection continuum robot with follow-the-leader motion," *Int. J. Comput. Assist. Radiol. Surg.*, vol. 14, no. 11, pp. 2021–2029, Nov. 2019.
- [195] G. Dwyer, F. Chadebecq, M. T. Amo, C. Bergeles, E. Maneas, V. Pawar, E. V. Poorten, J. Deprest, S. Ourselin, P. De Coppi, T. Vercauteren, and D. Stoyanov, "A continuum robot and control interface for surgical assist in fetoscopic interventions," *IEEE Robot. Autom. Lett.*, vol. 2, no. 3, pp. 1656–1663, Jul. 2017.
- [196] S. Song, Z. Li, M. Q.-H. Meng, H. Yu, and H. Ren, "Real-time shape estimation for wire-driven flexible robots with multiple bending sections based on quadratic Bézier curves," *IEEE Sensors J.*, vol. 15, no. 11, pp. 6326–6334, Nov. 2015.
- [197] S. Tully, G. Kantor, M. A. Zenati, and H. Choset, "Shape estimation for image-guided surgery with a highly articulated snake robot," in *Proc. IEEE/RSJ Int. Conf. Intell. Robots Syst.*, Sep. 2011, pp. 1353–1358.
- [198] J. Back, L. Lindenroth, K. Rhode, and H. Liu, "Model-free position control for cardiac ablation catheter steering using electromagnetic position tracking and tension feedback," *Frontiers Robot. AI*, vol. 4, p. 17, May 2017.
- [199] S. Song, H. Ge, J. Wang, and M. Q.-H. Meng, "Real-time multiobject magnetic tracking for multi-arm continuum robots," *IEEE Trans. Instrum. Meas.*, vol. 70, pp. 1–9, 2021.
- [200] C. E. Campanella, A. Cuccovillo, C. Campanella, A. Yurt, and V. M. N. Passaro, "Fibre Bragg grating based strain sensors: Review of technology and applications," *Sensors*, vol. 18, no. 9, p. 3115, Sep. 2018.
- [201] J. Liu, J. Zhang, X. Li, and Z. Zheng, "Study on multiplexing ability of identical fiber Bragg gratings in a single fiber," *Chin. J. Aeronaut.*, vol. 24, no. 5, pp. 607–612, Oct. 2011.
- [202] F. Khan, A. Denasi, D. Barrera, J. Madrigal, S. Sales, and S. Misra, "Multi-core optical fibers with Bragg gratings as shape sensor for flexible medical instruments," *IEEE Sensors J.*, vol. 19, no. 14, pp. 5878–5884, Jul 2019
- [203] F. Khan, A. Donder, S. Galvan, F. R. Y. Baena, and S. Misra, "Pose measurement of flexible medical instruments using fiber Bragg gratings in multi-core fiber," *IEEE Sensors J.*, vol. 20, no. 18, pp. 10955–10962, Sep. 2020.

- [204] S. Jäckle, T. Eixmann, H. Schulz-Hildebrandt, G. Hüttmann, and T. Pätz, "Fiber optical shape sensing of flexible instruments for endovascular navigation," *Int. J. Comput. Assist. Radiol. Surg.*, vol. 14, no. 12, pp. 2137–2145, Dec. 2019.
- [205] Y. Chitalia, N. J. Deaton, S. Jeong, N. Rahman, and J. P. Desai, "Towards FBG-based shape sensing for micro-scale and meso-scale continuum robots with large deflection," *IEEE Robot. Autom. Lett.*, vol. 5, no. 2, pp. 1712–1719, Apr. 2020.
- [206] S. C. Ryu and P. E. Dupont, "FBG-based shape sensing tubes for continuum robots," in *Proc. IEEE Int. Conf. Robot. Autom. (ICRA)*, May 2014, pp. 3531–3537.
- [207] N. Rahman, N. J. Deaton, J. Sheng, S. S. Cheng, and J. P. Desai, "Modular FBG bending sensor for continuum neurosurgical robot," *IEEE Robot. Autom. Lett.*, vol. 4, no. 2, pp. 1424–1430, Apr. 2019.
- [208] F. Alambeigi, M. Bakhtiarinejad, A. Azizi, R. Hegeman, I. Iordachita, H. Khanuja, and M. Armand, "Inroads toward robot-assisted internal fixation of bone fractures using a bendable medical screw and the curved drilling technique," in *Proc. 7th IEEE Int. Conf. Biomed. Robot. Biomechatronics (Biorob)*, Aug. 2018, pp. 595–600.
- [209] F. Alambeigi, Y. Wang, R. J. Murphy, I. Iordachita, and M. Armand, "Toward robot-assisted hard osteolytic lesion treatment using a continuum manipulator," in *Proc. 38th Annu. Int. Conf. IEEE Eng. Med. Biol.* Soc. (EMBC), Aug. 2016, pp. 5103–5106.
- [210] F. Alambeigi, Y. Wang, S. Sefati, C. Gao, Ryan. J. Murphy, I. Iordachita, R. H. Taylor, H. Khanuja, and M. Armand, "A curved-drilling approach in core decompression of the femoral head osteonecrosis using a continuum manipulator," *IEEE Robot. Autom. Lett.*, vol. 2, no. 3, pp. 1480–1487, Jul. 2017.
- [211] F. Alambeigi, M. Bakhtiarinejad, S. Sefati, R. Hegeman, I. Iordachita, H. Khanuja, and M. Armand, "On the use of a continuum manipulator and a bendable medical screw for minimally invasive interventions in orthopedic surgery," *IEEE Trans. Med. Robot. Bionics*, vol. 1, no. 1, pp. 14–21, Feb. 2019.
- [212] G. Amirkhani, A. Goodridge, M. Esfandiari, H. Phalen, J. H. Ma, I. Iordachita, and M. Armand, "Design and fabrication of a fiber Bragg grating shape sensor for shape reconstruction of a continuum manipulator," *IEEE Sensors J.*, vol. 23, no. 12, pp. 12915–12929, Jun. 2023.
- [213] Y. Dai, S. Wang, X. Wang, and H. Yuan, "A novel friction measuring method and its application to improve the static modeling accuracy of cable-driven continuum manipulators," *IEEE Robot. Autom. Lett.*, vol. 9, no. 4, pp. 3259–3266, Apr. 2024.
- [214] Y. Yi, J.-H. Youn, J.-S. Kim, D.-S. Kwon, and K.-U. Kyung, "Real-time shape estimation of hyper-redundant flexible manipulator using coiled fiber sensors," *Soft Robot.*, vol. 11, no. 5, pp. 821–834, Oct. 2024.
- [215] T. Li, L. Qiu, and H. Ren, "Distributed curvature sensing and shape reconstruction for soft manipulators with irregular cross sections based on parallel dual-FBG arrays," *IEEE/ASME Trans. Mechatronics*, vol. 25, no. 1, pp. 406–417, Feb. 2020.
- [216] S. Sefati, C. Gao, I. Iordachita, R. H. Taylor, and M. Armand, "Data-driven shape sensing of a surgical continuum manipulator using an uncalibrated fiber Bragg grating sensor," *IEEE Sensors J.*, vol. 21, no. 3, pp. 3066–3076, Feb. 2021.
- [217] X. T. Ha, D. Wu, M. Ourak, G. Borghesan, J. Dankelman, A. Menciassi, and E. V. Poorten, "Shape sensing of flexible robots based on deep learning," *IEEE Trans. Robot.*, vol. 39, no. 2, pp. 1580–1593, Apr. 2023.
- [218] K. Wang, Y. Mizuno, X. Dong, W. Kurz, M. Köhler, P. Kienle, H. Lee, M. Jakobi, and A. W. Koch, "Multimode optical fiber sensors: From conventional to machine learning-assisted," *Meas. Sci. Technol.*, vol. 35, no. 2, 2024, Art. no. 022002.
- [219] A. Schwarz, A. Mehrfard, G. Amirkhani, H. Phalen, J. H. Ma, R. B. Grupp, A. M. Gomez, and M. Armand, "Uncertainty-aware shape estimation of a surgical continuum manipulator in constrained environments using fiber Bragg grating sensors," in *Proc. IEEE Int. Conf. Robot. Autom. (ICRA)*, May 2024, pp. 5913–5919.
- [220] Z. Zhang, J. Dequidt, J. Back, H. Liu, and C. Duriez, "Motion control of cable-driven continuum catheter robot through contacts," *IEEE Robot. Autom. Lett.*, vol. 4, no. 2, pp. 1852–1859, Apr. 2019.
- [221] L. Cercenelli, B. Bortolani, and E. Marcelli, "CathROB: A highly compact and versatile remote catheter navigation system," *Appl. Bionics Biomechanics*, vol. 2017, pp. 1–13, Jan. 2017.



- [222] A. Gao, Z. Lin, C. Zhou, X. Ai, B. Huang, W. Chen, and G.-Z. Yang, "Body contact estimation of continuum robots with tensionprofile sensing of actuation fibers," *IEEE Trans. Robot.*, vol. 40, pp. 1492–1508, 2024.
- [223] R. Xu, A. Yurkewich, and R. V. Patel, "Curvature, torsion, and force sensing in continuum robots using helically wrapped FBG sensors," *IEEE Robot. Autom. Lett.*, vol. 1, no. 2, pp. 1052–1059, Jul. 2016.
- [224] Q. Liu, Y. Dai, M. Li, B. Yao, and J. Zhang, "FBG-based sensorized surgical instrument for force measurement in minimally invasive robotic surgery," *IEEE Sensors J.*, vol. 24, no. 7, pp. 11450–11458, Apr. 2024.
- [225] F. Khan, R. J. Roesthuis, and S. Misra, "Force sensing in continuum manipulators using fiber Bragg grating sensors," in *Proc. IEEE/RSJ Int. Conf. Intell. Robots Syst. (IROS)*, Sep. 2017, pp. 2531–2536.
- [226] P. Sincak, E. Prada, L. Miková, R. Mykhailyshyn, M. Varga, T. Merva, and I. Virgala, "Sensing of continuum robots: A review," *Sensors*, vol. 24, no. 4, p. 1311, Feb. 2024.
- [227] L. Wang, C. Zhou, Y. Cao, R. Zhao, and K. Xu, "Vision-based markerless tracking for continuum surgical instruments in robot-assisted minimally invasive surgery," *IEEE Robot. Autom. Lett.*, vol. 8, no. 11, pp. 7202–7209, Nov. 2023.
- [228] L. Sciavicco and B. Siciliano, "Modelling and control of robot manipulators," Meas. Sci. Technol., vol. 11, no. 12, p. 1828, 2000.
- [229] J. Son, H. Kang, and S. H. Kang, "A review on robust control of robot manipulators for future manufacturing," *Int. J. Precis. Eng. Manuf.*, vol. 24, no. 6, pp. 1083–1102, Jun. 2023.
- [230] N. Simaan, R. M. Yasin, and L. Wang, "Medical technologies and challenges of robot-assisted minimally invasive intervention and diagnostics," *Annu. Rev. Control, Robot., Auto. Syst.*, vol. 1, no. 1, pp. 465–490, May 2018.
- [231] T. da Veiga, J. H. Chandler, P. Lloyd, G. Pittiglio, N. J. Wilkinson, A. K. Hoshiar, R. A. Harris, and P. Valdastri, "Challenges of continuum robots in clinical context: A review," *Prog. Biomed. Eng.*, vol. 2, no. 3, Aug. 2020, Art. no. 032003.
- [232] F. Janabi-Sharifi, A. Jalali, and I. D. Walker, "Cosserat rod-based dynamic modeling of tendon-driven continuum robots: A tutorial," *IEEE Access*, vol. 9, pp. 68703–68719, 2021.
- [233] C. Della Santina, C. Duriez, and D. Rus, "Model-based control of soft robots: A survey of the state of the art and open challenges," *IEEE Control Syst.*, vol. 43, no. 3, pp. 30–65, Jun. 2023.
- [234] R. J. Murphy, M. D. M. Kutzer, S. M. Segreti, B. C. Lucas, and M. Armand, "Design and kinematic characterization of a surgical manipulator with a focus on treating osteolysis," *Robotica*, vol. 32, no. 6, pp. 835–850, Sep. 2014.
- [235] Y. Gao, K. Takagi, T. Kato, N. Shono, and N. Hata, "Continuum robot with follow-the-leader motion for endoscopic third ventriculostomy and tumor biopsy," *IEEE Trans. Biomed. Eng.*, vol. 67, no. 2, pp. 379–390, Feb. 2020.
- [236] T. Kato, F. King, K. Takagi, and N. Hata, "Robotized catheter with enhanced distal targeting for peripheral pulmonary biopsy," *IEEE/ASME Trans. Mechatronics*, vol. 26, no. 5, pp. 2451–2461, Oct. 2021.
- [237] V. K. Venkiteswaran, J. Sikorski, and S. Misra, "Shape and contact force estimation of continuum manipulators using pseudo rigid body models," *Mechanism Mach. Theory*, vol. 139, pp. 34–45, Sep. 2019.
- [238] Y. Huang, Q. Zhao, J. Hu, and H. Liu, "Design and modeling of a multi-DoF magnetic continuum robot with diverse deformation modes," *IEEE Robot. Autom. Lett.*, vol. 9, no. 4, pp. 3956–3963, Apr. 2024.
- [239] T. Mahl, A. E. Mayer, A. Hildebrandt, and O. Sawodny, "A variable curvature modeling approach for kinematic control of continuum manipulators," in *Proc. Amer. Control Conf.*, Jun. 2013, pp. 4945–4950.
- [240] D. B. Camarillo, C. F. Milne, C. R. Carlson, M. R. Zinn, and J. K. Salisbury, "Mechanics modeling of tendon-driven continuum manipulators," *IEEE Trans. Robot.*, vol. 24, no. 6, pp. 1262–1273, Dec. 2008.
- [241] R. Peng, Y. Wang, and P. Lu, "A tendon-driven continuum manipulator with robust shape estimation by multiple IMUs," *IEEE Robot. Autom. Lett.*, vol. 9, no. 4, pp. 3084–3091, Apr. 2024.
- [242] A. Sayadi, R. Cecere, and A. Hooshiar, "Finite arc method: Fast-solution extended piecewise constant curvature model of soft robots with large variable curvature deformations," *Robot. Rep.*, vol. 2, no. 1, pp. 49–64, Mar. 2024
- [243] A. A. Alqumsan, S. Khoo, and M. Norton, "Robust control of continuum robots using Cosserat rod theory," *Mechanism Mach. Theory*, vol. 131, pp. 48–61, Jan. 2019.

- [244] P. S. Gonthina, A. D. Kapadia, I. S. Godage, and Ian. D. Walker, "Modeling variable curvature parallel continuum robots using Euler curves," in *Proc. Int. Conf. Robot. Autom. (ICRA)*, May 2019, pp. 1679–1685.
- [245] P. Rao, Q. Peyron, and J. Burgner-Kahrs, "Using Euler curves to model continuum robots," in *Proc. IEEE Int. Conf. Robot. Autom. (ICRA)*, May 2021, pp. 1402–1408.
- [246] X. J. Zheng, M. Ding, L. X. Liu, L. Wang, and Y. Guo, "Static-to-kinematic modeling and experimental validation of tendon-driven quasi continuum manipulators with nonconstant subsegment stiffness," *Chin. Phys. B*, vol. 33, no. 1, Jan. 2024, Art. no. 010703.
- [247] L. Jiajia, D. Fuxin, L. Yibin, L. Yanqiang, Z. Tao, and Z. Gang, "A novel inverse kinematics algorithm using the Kepler oval for continuum robots," *Appl. Math. Model.*, vol. 93, pp. 206–225, May 2021.
- [248] S. Grazioso, G. Di Gironimo, and B. Siciliano, "From differential geometry of curves to helical kinematics of continuum robots using exponential mapping," in *Advances in Robot Kinematics*. Cham, Switzerland: Springer, 2018.
- [249] A. L. Orekhov, E. Z. Ahronovich, and N. Simaan, "Lie group formulation and sensitivity analysis for shape sensing of variable curvature continuum robots with general string encoder routing," *IEEE Trans. Robot.*, vol. 39, no. 3, pp. 2308–2324, Jun. 2023.
- [250] M. Hayati and M. Turkseven, "Shape reconstruction of a soft actuator based on Bezier curves using soft strain sensors," in *Proc. IEEE 7th Int. Conf. Soft Robot. (RoboSoft)*, Apr. 2024, pp. 977–982.
- [251] F. Xu, Y. Zhang, J. Sun, and H. Wang, "Adaptive visual servoing shape control of a soft robot manipulator using Bézier curve features," *IEEE/ASME Trans. Mechatronics*, vol. 28, no. 2, pp. 945–955, Apr. 2023.
- [252] Z. Mu, Y. Chen, Z. Li, C. Wang, N. Ding, and H. Qian, "A combined planning method based on biarc curve and Bézier curve for concentric cable-driven manipulators working in confined environments," *IEEE/ASME Trans. Mechatronics*, vol. 27, no. 6, pp. 4475–4486, Dec. 2022.
- [253] H. Yuan, P. W. Y. Chiu, and Z. Li, "Shape-reconstruction-based force sensing method for continuum surgical robots with large deformation," *IEEE Robot. Autom. Lett.*, vol. 2, no. 4, pp. 1972–1979, Oct. 2017.
- [254] L. Piegl and W. Tiller, *The NURBS Book*. Berlin, Germany: Springer, 1996.
- [255] B. Jones and I. Walker, "Three-dimensional modeling and display of continuum robots," in *Proc. IEEE/RSJ Int. Conf. Intell. Robots Syst.*, Oct. 2006, pp. 5872–5877.
- [256] Z. Li, J. Dankelman, and E. De Momi, "Path planning for endovascular catheterization under curvature constraints via two-phase searching approach," *Int. J. Comput. Assist. Radiol. Surg.*, vol. 16, no. 4, pp. 619–627, Apr. 2021.
- [257] S. Luo, M. Edmonds, J. Yi, X. Zhou, and Y. Shen, "Spline-based modeling and control of soft robots," in *Proc. IEEE/ASME Int. Conf. Adv. Intell. Mechatronics (AIM)*, Jul. 2020, pp. 482–487.
- [258] C. Armanini, F. Boyer, A. T. Mathew, C. Duriez, and F. Renda, "Soft robots modeling: A structured overview," *IEEE Trans. Robot.*, vol. 39, no. 3, pp. 1728–1748, Jun. 2023.
- [259] R. T. Farouki, C. Giannelli, and A. Sestini, "New developments in theory, algorithms, and applications for pythagorean-hodograph curves," in *Advanced Methods for Geometric Modeling and Numerical Simulation*, C. Giannelli and H. Speleers, Eds., Cham, Switzerland: Springer, 2019, pp. 77–127.
- [260] S. Mbakop, G. Tagne, S. V. Drakunov, and R. Merzouki, "Parametric PH curves model based kinematic control of the shape of mobile soft manipulators in unstructured environment," *IEEE Trans. Ind. Electron.*, vol. 69, no. 10, pp. 10292–10300, Oct. 2022.
- [261] I. Singh, Y. Amara, A. Melingui, P. Mani Pathak, and R. Merzouki, "Modeling of continuum manipulators using Pythagorean hodograph curves," *Soft Robot.*, vol. 5, no. 4, pp. 425–442, Aug. 2018.
- [262] H. Guo, F. Ju, D. Bai, X. Wei, L. Wang, and B. Chen, "Shape reconstruction for continuum robot based on Pythagorean Hodograph–Bézier curve with IMU and vision sensors," *IEEE Sensors J.*, vol. 23, no. 8, pp. 8535–8544, Apr. 2023.
- [263] S. Mbakop, G. Tagne, T. Chevillon, S. V. Drakunov, and R. Merzouki, "PH-Gauss-Lobatto reduced-order-model for shape control of softcontinuum manipulators," *IEEE Trans. Robot.*, vol. 40, pp. 2641–2655, 2024.



- [264] V. Falkenhahn, T. Mahl, A. Hildebrandt, R. Neumann, and O. Sawodny, "Dynamic modeling of bellows-actuated continuum robots using the Euler-Lagrange formalism," *IEEE Trans. Robot.*, vol. 31, no. 6, pp. 1483–1496, Dec. 2015.
- [265] B. He, Z. Wang, Q. Li, H. Xie, and R. Shen, "An analytic method for the kinematics and dynamics of a multiple-backbone continuum robot," *Int. J. Adv. Robotic Syst.*, vol. 10, no. 1, p. 84, Jan. 2013.
- [266] G. D. Giudice, A. L. Orekhov, J.-H. Shen, K. M. Joos, and N. Simaan, "Investigation of micromotion kinematics of continuum robots for volumetric OCT and OCT-guided visual servoing," *IEEE/ASME Trans. Mechatronics*, vol. 26, no. 5, pp. 2604–2615, Oct. 2021.
- [267] J. Yang, E. Harsono, and H. Yu, "Dynamic modeling and validation of a hybrid-driven continuum robot with antagonistic mechanisms," *Mechanism Mach. Theory*, vol. 197, Jul. 2024, Art. no. 105635.
- [268] R. Roy, L. Wang, and N. Simaan, "Investigation of effects of dynamics on intrinsic wrench sensing in continuum robots," in *Proc. IEEE Int. Conf. Robot. Autom. (ICRA)*, May 2016, pp. 2052–2059.
- [269] W. Ai, X. Lin, Y. Luo, and X. Wang, "Fractional-order modeling and identification for an SCR denitrification process," *Fractal Fractional*, vol. 8, no. 9, p. 524, Sep. 2024.
- [270] F. Boyer, V. Lebastard, F. Candelier, and F. Renda, "Dynamics of continuum and soft robots: A strain parameterization based approach," *IEEE Trans. Robot.*, vol. 37, no. 3, pp. 847–863, Jun. 2021.
- [271] H. Li, L. Xun, and G. Zheng, "Piecewise linear strain Cosserat model for soft slender manipulator," *IEEE Trans. Robot.*, vol. 39, no. 3, pp. 2342–2359, Jun. 2023.
- [272] S. M. Mustaza, Y. Elsayed, C. Lekakou, C. Saaj, and J. Fras, "Dynamic modeling of fiber-reinforced soft manipulator: A visco-hyperelastic material-based continuum mechanics approach," *Soft Robot.*, vol. 6, no. 3, pp. 305–317, Jun. 2019.
- [273] M. Tummers, V. Lebastard, F. Boyer, J. Troccaz, B. Rosa, and M. T. Chikhaoui, "Cosserat rod modeling of continuum robots from Newtonian and Lagrangian perspectives," *IEEE Trans. Robot.*, vol. 39, no. 3, pp. 2360–2378, Jun. 2023.
- [274] S. M. H. Sadati, S. E. Naghibi, A. Shiva, B. Michael, L. Renson, M. Howard, C. D. Rucker, K. Althoefer, T. Nanayakkara, S. Zschaler, C. Bergeles, H. Hauser, and I. D. Walker, "TMTDyn: A MATLAB package for modeling and control of hybrid rigid–continuum robots based on discretized lumped systems and reduced-order models," *Int. J. Robot. Res.*, vol. 40, no. 1, pp. 296–347, Jan. 2021.
- [275] D. C. Rucker and R. J. Webster, "Mechanics of continuum robots with external loading and general tendon routing," in *Experimental Robotics*, O. Khatib, V. Kumar, and G. Sukhatme, Eds., Berlin, Germany: Springer, 2014, pp. 645–654.
- [276] L. Qin, H. Peng, X. Huang, M. Liu, and W. Huang, "Modeling and simulation of dynamics in soft robotics: A review of numerical approaches," *Current Robot. Rep.*, vol. 5, no. 1, pp. 1–13, Aug. 2023.
- [277] L. Xun, G. Zheng, and A. Kruszewski, "Cosserat-rod-based dynamic modeling of soft slender robot interacting with environment," *IEEE Trans. Robot.*, vol. 40, pp. 2811–2830, 2024.
- [278] P. E. Dupont, J. Lock, B. Itkowitz, and E. Butler, "Design and control of concentric-tube robots," *IEEE Trans. Robot.*, vol. 26, no. 2, pp. 209–225, Apr. 2010.
- [279] M. Tummers, F. Boyer, V. Lebastard, A. Offermann, J. Troccaz, B. Rosa, and M. T. Chikhaoui, "Continuum concentric push–pull robots: A Cosserat rod model," *Int. J. Robot. Res.*, vol. 4, no. 33, Sep. 2024, Art. no. 02783649241263366.
- [280] X. Wang and N. Rojas, "Cosserat rod modeling and validation for a soft continuum robot with self-controllable variable curvature," in *Proc. IEEE* 7th Int. Conf. Soft Robot. (RoboSoft), Apr. 2024, pp. 705–710.
- [281] S. Pourghasemi Hanza and H. Ghafarirad, "Mechanics of fiber-reinforced soft manipulators based on inhomogeneous Cosserat rod theory," *Mech. Adv. Mater. Struct.*, vol. 31, no. 15, pp. 3161–3173, Aug. 2024.
- [282] P. M. Kolahi and M. H. Korayem, "Investigation and improving modeling and control for continuum magnetic robots using Cosserat theories and optimal control," *Acta Mechanica*, vol. 235, no. 5, pp. 3095–3110, May 2024.
- [283] T. Bretl and Z. McCarthy, "Quasi-static manipulation of a Kirchhoff elastic rod based on a geometric analysis of equilibrium configurations," *Int. J. Robot. Res.*, vol. 33, no. 1, pp. 48–68, Jan. 2014.
- [284] D. C. Rucker and R. J. Webster III, "Statics and dynamics of continuum robots with general tendon routing and external loading," *IEEE Trans. Robot.*, vol. 27, no. 6, pp. 1033–1044, Dec. 2011.

- [285] J. Till, V. Aloi, K. E. Riojas, P. L. Anderson, R. J. Webster III, and C. Rucker, "A dynamic model for concentric tube robots," *IEEE Trans. Robot.*, vol. 36, no. 6, pp. 1704–1718, Dec. 2020.
- [286] G. Amirkhani, F. Farahmand, S. M. Yazdian, and A. Mirbagheri, "An extended algorithm for autonomous grasping of soft tissues during robotic surgery," *Int. J. Med. Robot. Comput. Assist. Surg.*, vol. 16, no. 5, pp. 1–15, Oct. 2020.
- [287] W. Li, X. Huang, L. Yan, H. Cheng, B. Liang, and W. Xu, "Force sensing and compliance control for a cable-driven redundant manipulator," IEEE/ASME Trans. Mechatronics, vol. 29, no. 1, pp. 777–788, Feb. 2024.
- [288] X. Wei, F. Ju, H. Guo, B. Chen, and H. Wu, "Modeling and control of cable-driven continuum robot used for minimally invasive surgery," *Proc. Inst. Mech. Eng.*, H, J. Eng. Med., vol. 237, no. 1, pp. 35–48, Jan. 2023.
- [289] K. Oliver-Butler, J. Till, and C. Rucker, "Continuum robot stiffness under external loads and prescribed tendon displacements," *IEEE Trans. Robot.*, vol. 35, no. 2, pp. 403–419, Apr. 2019.
- [290] V. Aloi, K. T. Dang, E. J. Barth, and C. Rucker, "Estimating forces along continuum robots," *IEEE Robot. Autom. Lett.*, vol. 7, no. 4, pp. 8877–8884, Oct. 2022.
- [291] J. M. Ferguson, D. C. Rucker, and R. J. Webster, "Unified shape and external load state estimation for continuum robots," *IEEE Trans. Robot.*, vol. 40, pp. 1813–1827, 2024.
- [292] L. Ding, L. Niu, Y. Su, H. Yang, G. Liu, H. Gao, and Z. Deng, "Dynamic finite element modeling and simulation of soft robots," *Chin. J. Mech. Eng.*, vol. 35, no. 1, p. 24, Dec. 2022.
- [293] O. Shamilyan, I. Kabin, Z. Dyka, O. Sudakov, A. Cherninskyi, M. Brzozowski, and P. Langendoerfer, "Intelligence and motion models of continuum robots: An overview," *IEEE Access*, vol. 11, pp. 60988–61003, 2023.
- [294] D. Wu, R. Zhang, A. Pore, D. Dall'Alba, X. T. Ha, Z. Li, Y. Zhang, F. Herrera, M. Ourak, W. Kowalczyk, E. De Momi, A. Casals, J. Dankelman, J. Kober, A. Menciassi, P. Fiorini, and E. Vander Poorten, "A review on machine learning in flexible surgical and interventional robots: Where we are and where we are going," *Biomed. Signal Process. Control*, vol. 93, Jul. 2024, Art. no. 106179.
- [295] X. Wang, Y. Li, and K.-W. Kwok, "A survey for machine learning-based control of continuum robots," *Frontiers Robot. AI*, vol. 8, Sep. 2021, Art. no. 730330.
- [296] J. Kołota and T. C. Kargin, "Comparison of various reinforcement learning environments in the context of continuum robot control," *Appl. Sci.*, vol. 13, no. 16, p. 9153, Aug. 2023.



**FAHAD IQBAL** (Graduate Student Member, IEEE) received the B.H.Sc. degree in biomedical sciences from the University of Calgary, Calgary, AB, Canada, in 2020, where he is currently pursuing the joint M.D. and Ph.D. degree in neuroscience.

He was a Research Student at Project neuroArm during his undergraduate. His research interests include surgical robotics, neuron-chip interfacing, epilepsy, anesthetics, and neurophysiology.



MOJTABA ESFANDIARI received the B.Sc. degree in mechanical engineering from the Amirkabir University of Technology (Tehran Polytechnic), Tehran, Iran, in 2014, and the M.Sc. degree in mechanical engineering from the Sharif University of Technology, Tehran, in 2017. He is currently pursuing the Ph.D. degree in mechanical engineering with Johns Hopkins University, Baltimore, MD, USA.

He was a Research Assistant at the Project neuof Calgary, Calgary, AB, Canada, from 2018 to 2021.

roArm, University of Calgary, Calgary, AB, Canada, from 2018 to 2021. His research interests include modeling, optimization, and control of surgical robotic systems.





**GOLCHEHR AMIRKHANI** received the B.Sc. degree in mechanical engineering from Shahid Beheshti University, Tehran, Iran, in 2015, and the M.Sc. degree in mechatronics from the Sharif University of Technology, Tehran, in 2018.

She is currently pursuing the Ph.D. degree in mechanical engineering with Johns Hopkins University, Baltimore, MD, USA. Her research interests include sensing and control of continuum manipulators with applications in surgical robotics and autonomous break systems.



**HAMIDREZA HOSHYARMANESH** received the B.Sc. and M.Sc. degrees in manufacturing engineering and industrial automation and the Ph.D. degree in mechanical engineering (mechatronics) from Isfahan University of Technology, Iran, in 2005, 2008, and 2015, respectively.

During the Ph.D. program, he joined the MC Laboratory, Yonsei University, Seoul, South Korea, as a Visiting Researcher, from 2012 to 2013. He was a Faculty Member, in 2010,

a Deputy of Research Affairs, and the Founder of the Mechatronics Laboratory, Islamic Azad University, Isfahan, Iran. He was formerly the Head of the Robohexapod Research Group, Isfahan Science and Technology Town. In 2015, he joined Project neuroArm, University of Calgary, as a Postdoctoral Research Fellow. Then, he served as the Chief Technology Officer at Orb-Surgical Ltd. and the Engineering Manager at Project neuroArm. He is also the Director of Operations at Skye Automation Inc. His research interests include mechatronics, surgical robotics, haptic hand controllers, structural health monitoring, piezoelectric sensors and actuators, industrial automation, and manufacturing processes.



**SANJU LAMA** received the Ph.D. degree from the Department of Clinical Neurosciences, University of Calgary, Calgary, AB, Canada.

She went on to obtain her concurrent fellowship in intra-operative MRI and integration of novel surgical technologies in the operating room (OR), including telerobotics. Her present pursuit remains the translation of evolving digital innovations and systems within the OR and healthcare sphere, with the intent of fostering standardized

health paradigms. Balancing academia in clinical neurosciences with a focus on technological innovation in neurosurgery, she currently serves as the Associate Director of Medical Robotics at Project neuroArm, University of Calgary, and the Chief Operating Officer of OrbSurgical Ltd. Her research interests include smart surgical devices, telerobotics, AI, interconnected systems, and their adoption within OR and health care.



**MAHDI TAVAKOLI** (Senior Member, IEEE) received the B.Sc. degree in electrical engineering from the Ferdowsi University of Mashhad, Mashhad, Iran, in 1996, the M.Sc. degree in electrical engineering from the K. N. Toosi University of Technology, Tehran, Iran, in 1999, and the Ph.D. degree in electrical and computer engineering from Western University, London, ON, Canada, in 2005.

In 2006, he was a Postdoctoral Researcher with Canadian Surgical Technologies and Advanced Robotics, Canada. From 2007 to 2008, he was an NSERC Postdoctoral Fellow with Harvard University, USA. He is currently a Professor with the Department of Electrical and Computer Engineering, University of Alberta, Canada. He is the lead author of the book *Haptics for Teleoperated Surgical Robotic Systems* (World Scientific, 2008). His research interest includes robotics and systems control. Specifically, his research focuses on haptics and teleoperation control, medical robotics, and image-guided surgery. He is an Associate Editor of IEEE/ASME Transactions on Mechatronics, *Journal of Medical Robotics Research, IET Control Theory and Applications*, and *Mechatronics*.



**GARNETTE R. SUTHERLAND** received the B.Sc. degree in chemistry and the M.D. degree from the University of Manitoba, Winnipeg, MB, Canada, in 1974 and 1978, respectively, and the F.R.C.S.C. degree from the University of Western Ontario, ON, Canada, in 1984.

He is currently a Professor of neurosurgery with the University of Calgary, Calgary, AB, Canada. He continues to advance medical robotics with a translational focus, with his current academic

interest spanning advanced haptics in medical robotics, molecular imaging with targeted contrast agents in traumatic brain injury and brain tumors, molecular characterization and vibration-based profiling of brain tumors, sensorized smart surgical tools technology, and virtual reality in surgical simulation. He has received multiple awards and recognitions, including American Astronautical Society-NASA Award for Earth Applications of Space Technology, induction into the Space Technology Hall of Fame, the NASA Technology Achievement Medal, and the Order of Canada.

. . .